STATE OF OREGON
DEPARTMENT OF GEOLOGY AND MINERAL INDUSTRIES
RUARRI J. DAY-STIRRAT, STATE GEOLOGIST
www.oregongeology.org

Geologic Map of the Athena 7.5′ Quadrangle, Umatilla County, Oregon

2023

GMS-129

Geologic Map of the Athena 7.5′ Quadrangle, Umatilla County, Oregon

Jason D. McClaughry[1] and Carlie J.M. Azzopardi[2]

Cartography by Jon J. Franczyk[2] and Geodatabase by Carlie J.M. Azzopardi[2]

[1]Oregon Department of Geology and Mineral Industries, Baker City Field Office, Baker County Courthouse, 1995 3rd Street, Suite 130, Baker City, OR 97814
[2]Oregon Department of Geology and Mineral Industries, 800 NE Oregon Street, Suite 965, Portland, OR 97232

Detailed geologic mapping in this part of the Walla Walla River basin is supported in part by a grant from the STATEMAP component of the U.S. Geological Survey (USGS) National Cooperative Geologic Mapping Program (NCGMP) under cooperative agreement G21AC00647. Additional funds were provided by the State of Oregon through the Oregon Department of Geology and Mineral Industries (DOGAMI).

PLATE 2

INTRODUCTION

The Athena 7.5′ quadrangle in Umatilla County of northeast Oregon includes an area of 135 square kilometers (km²) at the eastern edge of the Columbia Plateau, a broad depression forming the northwestern flank of the Blue Mountains (Figure 1). The oldest rocks in the map area are part of the ~17 to 6 Ma (mega annum) Columbia River Basalt Group (CRBG), a succession of tholeiitic basalt and basaltic andesite lava flows cropping out over more than 210,000 km² in parts of Washington, Oregon, Idaho, and Nevada (Plate 1; Figures 1 and 2; Reidel and others, 2013a). In the Athena 7.5′ quadrangle, the CRBG is locally intermittently overlain by upper Miocene and lower Pleistocene sedimentary rocks, a regionally widespread and thick blanket of lower Pleistocene to Holocene loess, and Upper Pleistocene and Holocene alluvial units on valley floors (Plate 1). Three major fault zones converge in this part of the Columbia Plateau, including the WNW-striking Wallula fault zone, NNW-striking Milton Freewater fault zone, and the NNE-striking Hite fault zone (Hooper and Conrey, 1989; Kuehn, 1995; Reidel and others, 2013b; Reidel and others, 2021; Madin and others, 2023; Figures 1 and 3).

The geology and structure of the Athena 7.5′ quadrangle was mapped by the Oregon Department of Geology and Mineral Industries (DOGAMI) between 2021 and 2022. Detailed geologic mapping in the Athena 7.5′ quadrangle is a high priority of the Oregon Geologic Map Advisory Committee, supported in part by grants from the STATEMAP component of the U.S. Geological Survey (USGS) National Cooperative Geologic Mapping Program (NCGMP) under cooperative agreement G21AC00647. Additional funds were provided by the State of Oregon through DOGAMI.

The chief objective of this investigation is to provide an updated and spatially accurate geologic framework for the area as part of a multiyear study of the geology of the larger Walla Walla River basin. Additional key objectives of this project are to: 1) map individual CRBG lava flows and crosscutting faults to determine flow distribution, fault offsets, and fault history in this part of the Walla Walla River basin of northeast Oregon; and 2) characterize the stratigraphic framework and geologic conditions controlling the distribution of water resources within the CRBG. CRBG-hosted aquifers provide a critical water supply in the map area and more widely across the Pacific Northwest (Piersol and Sprenke, 2015). New detailed geologic data presented here also provides a basis for future geologic, geohydrologic, and geohazard studies in the region.

Primary sources of map information consulted during this study include previous works by Hogenson (1964), Newcomb (1965), Walker (1973), Swanson and others (1981), Kuehn (1995), Hutter (1997), Ferns and others (2006 a, b), Derkey and others (2006), and Madin and Geitgey (2007). Soil information from Johnson and Makinson (1988) aided with mapping Quaternary surficial units. Additional sources of information are cited in the Explanation of Map Units and in the DataSourcePolys feature class in the geodatabase.

The core publication products of this study are a plottable geologic map and cross section (Plate 1), Esri ArcGIS™ geodatabase, and Microsoft Excel® spreadsheets tabulating point data for geochemistry, orientation points, and well data. The geodatabase presents new geologic mapping in a digital format consistent with the USGS NCGMP Map Schema (GeMS level 3; USGS NCGMP, 2020). It contains spatial information, including map unit polygons, contacts and faults, geologic lines, geochemistry points, orientation points, and well data, as well as data about each geologic unit such as age, lithology, mineralogy, and structure. Surficial and bedrock units in the geodatabase are depicted on Plate 1 at a scale of 1:24,000. Plate 1 includes: 1) a detailed geologic map showing the relationship of both bedrock and surficial units, including concealed bedrock contacts; 2) a simplified bedrock geologic map showing the distribution of contrasting bedrock lithologies and critical structural relationships; and 3) a geologic cross section labeled A-A′.

METHODS

Geologic mapping data in the Athena 7.5′ quadrangle was collected digitally using a GPS-enabled Apple® iPad® 4, loaded with Esri™ Collector, following standard DOGAMI procedures outlined in Duda and others (2018, 2019). Detailed field mapping used 1-meter (m) lidar DEMs (8 pts/m²), USGS 10-m DEMs, USGS digital raster graphics of traditional topographic maps, and digital Esri™ imagery as base maps. Fieldwork conducted during this study consisted of data collection along roads, combined with traverses across private lands mapping lithologic contacts and faults.

In this report, volcanic rocks with fine-grained (<1 mm; Mackenzie and others, 1997; Le Maitre and others, 2004) average crystal or particle size in the groundmass are characterized in the following manner:

- A coarse groundmass if the average crystal or particle size is <1 mm and can be determined using the naked eye (>~0.5 mm).
- A medium groundmass if crystals of average size cannot be determined by eye but can be distinguished by using a hand lens (>~0.05 mm).
- A fine groundmass if crystals or grains of average size can be determined only by using a microscope, or by hand lens recognition of sparkle or sheen in reflected light, indicating the presence of crystalline groundmass.
- A glassy groundmass if the groundmass has (fresh), or originally had (altered), groundmass with the characteristics of glass (e.g., conchoidal fracture; sharp, transparent edges; vitreous luster; etc.).
- Mixtures of crystalline and glassy groundmass are described as intersertal; ratios of glass to crystalline materials may be indicated by textural terms including holocrystalline, hypocrystalline, hyalophitic, hyalopilitic, and holohyaline.
- Microphenocrysts are defined as crystals larger than the overall groundmass and <1 mm across.

Whole-rock X-ray fluorescence (XRF) geochemical data are essential for separating difficult-to-distinguish CRBG lava flows. Many CRBG lava flows are too fine grained and glassy to be adequately characterized by mineralogical criteria alone and texturally similar appearing units may have meaningfully different chemical signatures. Whole-rock geochemical samples were prepared and analyzed by XRF at the Washington State University GeoAnalytical Lab, Pullman, Washington. Analytical procedures are described by Johnson and others (1999) and are available online at https://environment.wsu.edu/facilities/geoanalytical-lab/technical-notes/. Major element determinations are normalized to a 100 percent total on a volatile-free basis and recalculated with total iron expressed as FeOTotal (Tables 1 and 2).

Orientation measurements of geological planes (e.g., inclined bedding) were obtained in the field area by traditional compass and clinometer methods and compiled from data published by previous workers. Additional bedding measurements were generated using a routine and model developed by DOGAMI in Esri ArcGIS™ Model Builder to calculate three-point solutions from lidar bare-earth DEMs (Duda and others, 2018, 2019). Subsurface geology shown in the geologic cross section incorporates lithologic interpretations from water-well drill records located by the Oregon Water Resources Department (OWRD) GRID system (http://apps.wrd.state.or.us/apps/gw/well_log/; Plate 1). The geodatabases includes 32 located water-well logs with interpreted subsurface geologic units.

New mapping was compiled with published and unpublished data and converted into digital format using Esri ArcGIS™ ArcMAP™ GIS software. On-screen digitizing was performed through heads-up digitizing using a georeferenced hybrid 1-m lidar/USGS 10-m DEM, a 1:24,000-scale USGS DRGs of the Athena 7.5′ topographic quadrangle and the 2020 National Agriculture Imagery Program (NAIP) digital orthophoto for Umatilla County. The geologic time scale used is the 2022 (v2022/10), version of the International Stratigraphic Commission on Stratigraphy chronostratigraphic chart (https://stratigraphy.org/chart) revised from Gradstein and others (2004), Ogg and others (2008), and Cohen and others (2013). Colors given for hand sample descriptions are from the Geological Society of America Rock-Color Chart Committee (1991).

STRUCTURE

The structure of the Athena 7.5′ quadrangle consists of a thick section of broadly folded, horizontal to shallow NW-dipping (<5°), conformable CRBG lava flows that are cut by intersecting faults (Plate 1; Figure 3). Three major fault zones converge in this part of the Columbia Plateau, including the WNW-striking Wallula fault zone, NNW-striking Milton Freewater fault zone (Madin and others, 2023), and the NNE-striking Hite fault zone (Figures 1 and 3; Hooper and Conrey, 1989; Kuehn, 1995; Reidel and others, 2013b; Reidel and others, 2021). The Wallula fault zone is a set of locally active WNW-striking right-lateral strike-slip faults and N-S-striking normal faults mapped for ~120 km from Kennewick, Washington, through Milton Freewater, Oregon (Sherrod and others, 2016; Staisch and others, 2022). It parallels, and is an integral part of, the Olympic-Wallowa Lineament, an ~500-km-long collection of WNW-trending seismically active structural and physiographic features delineated between the Olympic Mountains of western Washington and the Blue Mountains of northeast Oregon (Raisz, 1945; Reidel and others, 2021). West and northwest of the Wallula fault zone strain in eastern Washington is accommodated along approximately east-west-trending folds in the Yakima Fold Belt (Figure 1; Staisch and others, 2022). East of Wallula Gap (WA) the Wallula fault zone transfers strain to the Hite fault zone across the intervening Milton Freewater fault zone (Blakely and others, 2014). The Milton Freewater fault zone is a complex zone of NNW-striking (avg. strike is N25°W) linear, vertical to subvertical, normal and right-lateral oblique-slip faults linking the Wallula fault zone on the north with the Hite fault zone on the southeast. Geologic mapping and analysis of high-resolution aeromagnetic data indicates this zone covers an ~40-km-wide swath between Wallula Gap (WA) on the west and Milton Freewater (OR) on the east. The Hite fault zone is defined by a 20- to 25-km-wide set of NNE-striking faults (avg. strike is N20°E), dominantly down-on-the-west, left-lateral oblique-slip faults, mapped for ~140 km between McKay Creek (OR) and Pomeroy (WA)(Kienle and others, 1979; Kendall, 1981; Personius and others, 1995). This zone of faulting is divided into four sections by Personius and others (1995) from northeast to southwest, including: 1) the Hite section; 2) the Kooskooskie section; 3) the Thorn Hollow section; and 4) the Agency section. Fault strands in the Hite fault zone are spatially coincident with and subparallel to the northeast-trending Klamath–Blue Mountain gravity-anomaly lineament, a major geophysical crustal feature recognized along the northwest slopes of the Blue Mountains (Figure 1; Riddihough and others, 1986; Wetzel and others, 2018).

Mapped faults in the Athena 7.5′ quadrangle cut the early to middle Miocene CRBG, with large-scale offset postdating the ~13.6 Ma Umatilla Member (**Tsu**)(Plate 1; Figure 3). Thickening or thinning of CRBG lava flows across faults is not apparent and all mapped units share a similar magnitude of displacement, suggesting largely post-CRBG faulting in the area. Age of latest offset along faults in the Athena 7.5′ quadrangle is unknown, as evidence for Quaternary movement has not been found.

Hite Fault Zone

Thorn Hollow and Saddle Hollow faults — The Thorn Hollow and Saddle Hollow faults are parallel, N10°E- to N20°E-striking left-lateral oblique-slip faults mapped along the eastern part of the Athena 7.5′ quadrangle (Plate 1; Figure 3; Kienle and others, 1979; Swanson and others, 1981). These two faults lie along the southwestern section of the more extensive Hite fault zone (Figure 3; Hooper and Conrey, 1989; Personius and others, 2003). Segments of the Thorn Hollow and Saddle Hollow faults have been mapped over a length of 45 km between Milton Freewater on the north and Calamity Creek on the south in the Cabbage Hill 7.5′ quadrangle (Figure 3; Kienle and others, 1979; Swanson and others, 1981; Ferns, 2006b; Ferns and McConnell, 2006). South of the Athena 7.5′ quadrangle, the Thorn Hollow and Saddle Hollow faults cut across the N70°E-striking Kanine Ridge fault zone, a major structural feature paralleled by the Umatilla River and forming part of the northern front of the Blue Mountains (Figure 3; Ferns, 2006b). On the north, in the vicinity of Dry Creek and Couse Creek, both the Thorn Hollow and Saddle Hollow faults terminate against N20°W- to N30°W-striking faults that are part of the Milton Freewater fault zone (Figure 3; Madin and others, 2023). Conspicuous NNE-trending topographic lineaments, recognized in USGS 10-m DEMs, 2020 NAIP orthophotos, and high-resolution aeromagnetic data (Blakely and others, 2020) correspond with both the Thorn Hollow and Saddle Hollow faults along their length (Figure 3). These topographic lineaments are expressed as an alignment of linear streams, saddles, and notches in ridges north of the Umatilla River. South of the Umatilla River a shallow, linear, vegetation-filled depression corresponds with the mapped faults (Kienle and others, 1979).

The Thorn Hollow and Saddle Hollow faults have been described as normal, left-lateral, and right-lateral strike-slip faults by Kienle and others (1979), Swanson and others (1981), Tolan and Reidel (1989), and Ferns (2006b). Detailed work in the eastern part of the larger Hite fault zone by Kuehn (1995) indicated left-lateral oblique-slip (down-on-the-northwest) on the main Hite fault (Figure 3). Reidel and others (1994) suggested left-lateral oblique-slip probably characterizes the entirety of the Hite fault zone.

Map pattern, three-point solutions on the mapped fault traces, and limited dip measurements (Kienle and others, 1979) indicate both the Thorn Hollow and Saddle Hollow faults have steeply NW-dipping fault attitudes between 80° and 85°NW. Both faults in the Athena 7.5′ quadrangle are portrayed as left-lateral oblique-slip faults, dominated by down-on-the-northwest slip along both strands. Segments of these faults bracketing Reed and Hawley Mountain in the southeast part of the Athena 7.5′ quadrangle are characterized by vertical down-on-the-northwest displacements of CRBG units by ~65 m across the Saddle Hollow fault and ~175 m across the Thorn Hollow fault (Plate 1, cross section A-A′). Northward along the Thorn Hollow fault in the Athena 7.5′ quadrangle, vertical, down-on-the-northwest offset is ~190 m east of Weston and ~150 m where the fault terminates against the Little Dry Creek fault 1 km south of Dry Creek (Plate 1; Figure 3). A similar sense of vertical, down-on-the-northwest offset is consistent along the entire length of the more persistent Thorn Hollow fault (Kienle and others, 1979; Swanson and others, 1981; Ferns, 2006b; Ferns and McConnell, 2006). By contrast, Ferns (2006b) recognized a transition to vertical, down-on-the-southeast offset along the Saddle Mountain fault south of Wildhorse Creek in the Thorn Hollow 7.5′ quadrangle (Figure 3).

Significant vertical displacement has also been accompanied by left-lateral horizontal displacement along the Saddle Hollow fault. Where the Saddle Hollow fault is mapped across Pine Creek, in the southeastern corner of the Athena 7.5′ quadrangle, the **Tgsmc**-**Tgww** contact is displaced ~150 m in a left-lateral horizontal sense (Plate 1). The horizontal motion is accompanied by 30 m of down-on-the-northwest vertical slip. Left-lateral horizontal slip along the Saddle Hollow fault is also suggested outside the map area. Where the Saddle Hollow fault crosses major canyons, the courses of major river drainages and their bounding canyons are commonly shifted in a conspicuous left-lateral sense (Figure 3). This type of left-lateral shift in ridge alignment is noted where the fault is crossed by Wildhorse Creek in the northeast corner of the Thorn Hollow 7.5′ quadrangle and Little Dry Creek and Dry Creek in the western part of the Weston Mountain 7.5′ quadrangle (Figure 3). Drag folding of CRBG units adjacent to the Saddle Hollow fault, north of the Little Dry Creek fault, has resulted in dips up to 15°NW. These steep dips contrast with the low dip angles of the CRBG (0 to 5°NW) where units are adjacent to the Dry Creek fault (Plate 1). A sense of strike-slip displacement is less certain for the Thorn Hollow fault, but may be recognized in the southernmost part of the Athena 7.5′ quadrangle where Wildhorse Creek is obliquely curved in a left-lateral sense across the mapped fault trace.

In the map area, the Thorn Hollow and Saddle faults bracket a number of generally NW-striking faults described below:

Wildhorse Road Fault — The Wildhorse Road fault is an entirely concealed N40°W- to N80°W-striking fault inferred to underly Wildhorse Creek in the southeast corner of the Athena 7.5′ quadrangle (Plate 1; Swanson and others, 1981). Mapping of CRBG lava flows across Wildhorse Creek suggests a structure with ~18 m of up-on-the-north vertical offset.

Schiewe Lane Fault — The Schiewe Lane fault is a 3-km-long, N0°W- to N5°W-striking normal fault mapped between the NW-striking Little Dry Creek fault and the NW-striking Hay Creek fault, north of Weston Mountain (Plate 1; Figure 3). Map pattern and a three-point solution on the mapped fault trace indicates the fault dips ~60°W. Normal, down-on-the-west vertical offset of ~80 m across the fault places lava flows of the Frenchman Springs Member (**Twfsl**, **Twfsh**, **Twfh**) on the west next to lava flows of the Sentinel Bluffs Member (**Tgsmu**, **Tgsmc**) on the east (Plate 1; Figure 2).

Milton Freewater fault zone

Spring Hollow Fault — The Spring Hollow fault is an entirely concealed N65°W-striking normal fault mapped in the southwestern part of the Athena 7.5′ quadrangle and northwest to Wildhorse Creek in the Adams 7.5′ quadrangle (Plate 1; Figure 3). Evidence for a concealed fault in this area includes mapped apparent down-on-the-southwest offset placing the Basalt of Umatilla (**Tsu**) on the southwest adjacent to the Basalt of Sentinel Gap (**Twfsl**) on the northeast and correspondence with a conspicuous WNW-trending aeromagnetic lineament (Plate 1; Figures 2 and 3b; Blakely and others, 2020b). Map pattern and a three-point solution indicates a southwest-dipping (~65° SW) fault with a down-on-the-southwest sense of vertical offset. The amount of vertical offset across the fault is unknown.

Pambrun Road Fault — The Pambrun Road fault is an entirely concealed N- to N15°W-striking normal fault mapped in the southwest corner of the Athena 7.5′ quadrangle (Plate 1; Figure 3). Evidence for a concealed fault in this area includes mapped down-on-the-west offset placing the Basalt of Umatilla (**Tsu**) on the west adjacent to the Basalt of Sentinel Gap (**Twfsl**) on the east, and correspondence with a NNW-trending aeromagnetic lineament and a NNW-trending topographic lineament visible in 1-m lidar DEMs (Plate 1; Figures 2 and 3b; Blakely and others, 2020b). Map pattern and a three-point solution indicates a vertical to steeply southwest-dipping (~75° to 80°SW) fault with a down-on-the-southwest sense of vertical offset. The amount of vertical offset across the fault is unknown. A component of right-lateral horizontal slip may be inferred because of apparent right-lateral topographic offset of the ridgeline south of Athena.

Wildhorse Creek Fault — The Wildhorse Creek fault is an entirely concealed N25°W-striking normal fault mapped beneath Wildhorse Creek and Athena in the southwestern part of the Athena 7.5′ quadrangle (Plate 1; Figure 3; Swanson and others, 1981). Mapping by Swanson and others (1981) indicated the fault may extend another 10 km northwest of Athena to Waterman. Evidence for a concealed fault in this area includes mapped offset of CRBG stratigraphy from northeast to southwest across Wildhorse Creek, apparent offset of CRBG flow stratigraphy in water wells UMAT 1462 and UMAT 57710, and a NNW-trending lineament observed in high-resolution aeromagnetic data (Plate 1; Figure 3; Blakely and others, 2020a, b). The Wildhorse Creek fault was also recognized as a negative anomaly in high-resolution aeromagnetic data extracted along a ground transect by Staisch and others (2022).

Based upon the inferred surface alignment of the Wildhorse Creek fault combined with geochemical fingerprinting of CRBG lava flows in water well UMAT 57710 ($n = 14$ samples; map nos. G31 to G44; Table 2), we project an ~80° SW.-dipping fault plane (apparent dip in cross section is 65°SW) to intersect the well at a depth interval between 409 m and 418 m, where the log describes blue clay seams and broken decomposed rock (Plate 1, cross section A-A′). Beneath the lower contact of the Basalt of McCoy Canyon (**Tgsmc**) at 354 m depth (sample UMAT 57710-1110), five samples from intervals 360 m, 391 m, 433 m, 463 m, and 476 m show a series of high-titanium/low-magnesium basaltic andesite lava flows (Table 2). Apparent stratigraphic position and geochemistry suggest a permissible assignment of these samples to the Winter Water Member (**Tgww**). However, if not repeated by faults, the assignment of these samples exclusively to the Winter Water Member (**Tgww**) would require that lava flow sequence to be as much as 122-m-thick, double the observed outcrop unit thickness of 52 m in the Athena 7.5′ quadrangle (Plate 1, cross section A-A′). To account for this observation, we correlate samples UMAT 57710-1180 and UMAT 57710-1281 with the Winter Water Member (**Tgww**), and samples collected below our projected fault with the Buttermilk Canyon member (**Tgbc**; samples UMAT 57710-1420 and UMAT 57710-1520) and Wapshilla Ridge Member (**Tgu**; sample UMAT 57710-1560)(Plate 1, cross section A-A′; Figure 2; Table 2). This lower lava flow sequence, interpreted in water well UMAT 57710, is consistent with Grande Ronde Basalt geochemical stratigraphy reported by Ferns (2006b) along the Umatilla River in the Thorn Hollow 7.5′ quadrangle (Figure 3a). The Wildhorse Creek fault is thus interpreted as an ~80°SW-dipping normal fault with a vertical, down-on-the-southwest offset of the CRBG section by ~60 m (Plate 1, cross section A-A′).

The SW-dipping Wildhorse Creek fault is also likely intersected by well UMAT 1462 just west of the confluence of Wildhorse and Eagle creeks in the southern part of the Athena 7.5′ quadrangle. At a depth interval of 27 to 116 m, the log describes a 30-m-thick section as 'broken rock', that we interpret as fault breccia. Geologic mapping suggests a vertical down-on-the-southwest offset of the Frenchman Springs Member (**Twfsl**, **Twfsh**, **Twfh**) by ~30 m across the fault in the southern part of the Athena 7.5′ quadrangle.

La Marr Gulch Fault — The La Marr Gulch fault is a N15°W-striking normal fault mapped for a length of 14 km from Athena on the south (Plate 1), across the southwest corner of the Milton Freewater 7.5′ quadrangle (Madin and others, 2023), northwest into the Waterman 7.5′ quadrangle (Figure 3a). At its southern mapped extent, the La Marr Gulch fault terminates against the ~N55°E-striking Weston fault (Plate 1; Figure 3). To the northeast, the La Marr Gulch fault intersects N70°W-striking faults in the Wallula fault zone (Figure 3; Madin and others, 2023). Map pattern, three-point solutions, and cross section interpretation of the La Marr Gulch fault in the Milton Freewater 7.5′ quadrangle indicates an ~85° NE-dipping normal fault with ~125 m of down-on-the-northeast vertical displacement of the **Tsu**-**Twfsl** contact (Figure 3; Madin and others, 2023, cross section D-D′).

Little Dry Creek Fault — The Little Dry Creek fault is a N40°W-striking right-lateral oblique-slip fault mapped for a length of 17 km from Weston Mountain on the southeast (Plate 1) to Pine Creek in the Milton Freewater 7.5′ quadrangle on the northwest (Figure 3; Swanson and others, 1981; Madin and others, 2023). To the northwest, the Little Dry Creek fault curves to a N55°W-striking alignment that merges with and parallels the Wallula fault zone (Figure 3; Madin and others, 2023). Map pattern and three-point solutions indicate an ~75° to 80° NE-dipping fault. Vertical, down-on-the-northeast offset of the **Tgsmu**-**Tgsmc** contact along Little Dry Creek, north of Weston Mountain in the eastern part of the Athena 7.5′ quadrangle, is ~17 m (Plate 1; Figure 3). Cross section interpretation of the Little Dry Creek fault in the Milton Freewater 7.5′ quadrangle indicates vertical, down-on-the-northeast displacement there of ~27 m (Madin and others, 2023, cross sections C-C′ and D-D′). Apparent right-lateral displacement along the Little Dry Creek fault along Little Dry Creek in the Athena 7.5′ quadrangle is on the order of 75 m (Plate 1).

Downing Fault — The Downing fault is a N25°W-striking right-lateral oblique-slip fault mapped for a length of 14 km between Heifer Creek in the Weston Mountain 7.5′ quadrangle on the southeast, through the northeast part of the Athena 7.5′ quadrangle (Plate 1), to Pine Creek in the Milton Freewater 7.5′ quadrangle (Figure 3; Swanson and others, 1981; Madin and others, 2023). At its northern extent, 1 km northwest of the confluence of Dry Hollow and Pine Creek, the Downing fault curves to a N55°W-N75°W-striking alignment that merges with and parallels the Wallula fault zone (Figure 3; Madin and others, 2023). Along Dry Creek, 2 km southeast of the map area, the Downing fault terminates against the north-northeast-striking Saddle Hollow fault (Figure 3). Map pattern and a three-point solution on the Downing fault, where it is mapped in the canyon wall west of OR Highway 11, indicate a fault plane dipping ~65°NE. Vertical, down-on-the-northeast displacement of the **Tsu**-**Twfsl** contact at the mouth of Little Dry Creek is ~20 m. Cross section interpretation along the length of the Downing fault in the Milton Freewater 7.5′ quadrangle suggests similar vertical, down-on-the-northeast displacement of ~15 to 20 m (Figure 3; Madin and others, 2023, cross sections D-D′ and E-E′). As the fault curves into alignment with the Wallula fault zone it becomes a more complex structure, with vertical, down-on-the-northeast offset as much 140 m (Madin and others, 2023, cross section C-C′). Right-lateral horizontal displacement along the southern part of the Downing fault, in the Athena 7.5′ quadrangle, is estimated at ~130 to 175 m, based on apparently offset CRBG lava flow contacts mapped from Downing east along Upper Dry Creek Road. The amount of horizontal displacement is uncertain north into the Milton Freewater 7.5′ quadrangle.

Blue Mountain Fault — The Blue Mountain fault is a N30°W- to N40°W-striking right-lateral oblique-slip fault mapped for a length of 11 km from Blue Mountain on the south (Plate 1), north beneath Dry Creek, to Barrett in the Milton Freewater 7.5′ quadrangle (Figure 3; Madin and others, 2023). At its northern extent, the Blue Mountain fault terminates against the E-W-striking Barrett fault (Figure 3; Madin and others, 2023). To the southeast, the fault ends against the Saddle Hollow fault. Map pattern and a three-point solution on the southern part of the fault indicate the fault dips ~65°SW. Cross section interpretation on the Blue Mountain fault from north to south indicates increasing vertical, down-on-the-southwest displacement of ~22 m south of Bade (**Tsu**-**Twfsl** contact) to ~100 m and ~139 m as the fault approaches the Barrett fault in the north (**Twfsl**-**Twfsh** contact) (Figure 3; Madin and others, 2023, cross sections C-C′, D-D′, and E-E′).

Dry Creek Fault — The Dry Creek fault is a N1°E-striking normal fault mapped for a length of 7 km between the confluence of Little Dry Creek and Dry Creek in the Athena 7.5′ quadrangle (Plate 1; Figure 4) north to Bade in the Milton Freewater 7.5′ quadrangle (Figure 3; Swanson and others, 1981; Madin and others, 2023). At its southern end, the Dry Creek fault is segmented by the Downing fault and links with the NW-striking Little Dry Creek fault (Plate 1; Figure 3). To the north, the fault links with the NW-striking Blue Mountain fault (Figure 3; Madin and others, 2023). The fault trace is mostly concealed along its length but is well exposed in a 12-m-high roadcut along OR Highway 11, 0.3 km south of Dry Creek (Plate 1; Figure 4). The OR Highway 11 roadcut exposes a 170-m-long section of the Basalt of Sentinel Gap (**Twfsh**), whose southwestern end is offset by several parallel, down-on-the-west normal fault strands, oriented N1°E, 56°NW (Figure 4). Fault strands enclose a 20-m-wide zone of fault-disturbed basalt. Thin, ≤2.5-cm-thick, veins of fracture-filling calcite and goethite line fault planes. Down-faulted basalt at the southwestern end of the outcrop is overlain unconformably by a 1- to 3-m-thick, channel-filling layer of moderately consolidated, poorly sorted conglomerate (**QTcg**) and a capping 0.5- to 3-m-thick layer of massive loess (**Qlo**)(Figure 4). Loess (**Qlo**) is pervasively cut by a stockwork of caliche veins, some of which extend ~0.5 m downward into fractured upper parts of the underlying basalt (**Twfsh**)(Figure 4).

The mapped distribution and apparent offset of the Umatilla Member (**Tsu**) and Basalt of Sentinel Gap (**Twfsl**, **Twfsh**) on either side of the Dry Creek fault suggests the possibility of several meters to as much as 20 m of down-on-the-west vertical displacement (Plate 1). The youngest geologic unit cut by the Dry Creek fault in the OR Highway 11 roadcut is the ~15.9 Ma Basalt of Sentinel Gap (**Twfsh**)(Figure 4). Kienle and others (1979) suggested the fault cut both conglomerate and overlying loess, with caliche-filled fractures extending upward along the fault through all exposed units. However, our analysis of the fault at the OR Highway 11 outcrop indicates that neither the conglomerate (**QTcg**) nor the loess (**Qlo**) is obviously cut by any of the fault stands. Instead, these units appear undeformed, draping the basalt and infilling low-lying areas above fault strands (Figure 4). Faulting along the Dry Creek fault therefore postdates the ~13.6 Ma Umatilla Member (**Tsu**); latest activity on the fault predates deposition of loess (**Qlo**) across the area after 1 to 2 Ma (McDonald and Busacca, 1988; Busacca, 1989).

Kienle and others (1979) described the Dry Creek fault, as designated here, as part of the more extensive Thorn Hollow fault. The Thorn Hollow fault and our Dry Creek fault are mapped separately in this report, as the two are divided from one another across the NW-striking Little Dry Creek fault (Plate 1; Figures 3 and 4). Accompanying this division is a noteworthy change in the amount of displacement on the two faults. South of the Little Dry Creek fault, vertical, down-on-the-west displacement on the Thorn Hollow fault is as much as 150 m, while north of the Little Dry Creek fault vertical, down-on-the-west displacement on the Dry Creek fault does not exceed 20 m (Plate 1).

Weston Fault — The Weston fault is an entirely concealed ~N55°E-striking normal fault striking obliquely across NNW-striking faults in the Milton Freewater fault zone. It is inferred to be present beneath loess (**Qlo**) for at least 9 km across the central part of the Athena 7.5′ quadrangle (Plate 1; Figure 3). The fault is suggested by: 1) a distinct NE-trending topographic break, visible in 1-m lidar DEMs, that is paralleled by OR Highway 11; 2) a similar NE-trending lineament and corresponding steep magnetic gradient observed in high-resolution aeromagnetic data (Blakely and others, 2020b); and 3) the widespread distribution of the plateau-capping Umatilla Member (**Tsu**) north of OR Highway 11 and limit of the unit to scattered upland areas south of the fault (Plate 1). Cross section interpretation suggests as much as 45 m of vertical, down-on-the-northwest offset of the CRBG across the Weston fault (Plate 1, cross section A-A′). Age of latest offset on the fault is unknown.

ACKNOWLEDGMENTS

Geologic mapping in the Athena 7.5′ quadrangle was supported through the STATEMAP component of the U.S. Geological Survey (USGS) National Cooperative Geologic Mapping Program under cooperative agreement G21AC00647. Additional funds were provided by the State of Oregon through the Oregon Department of Geology and Mineral Industries (DOGAMI). XRF geochemical analyses were prepared and analyzed by Dr. Ashley Steiner at the GeoAnalytical lab at Washington State University. The southern end of the Athena 7.5′ quadrangle includes lands of the Confederated Tribes of the Umatilla Indian Reservation (CTUIR). We appreciate permission to access and map across tribal lands. Field and logistical assistance from Kate Ely (CTUIR) and Christina Appleby (DOGAMI) is appreciated. Discussions with David Gaylord at Washington State University (WSU) improved our knowledge of regional loess deposits. Cartography for the map plates was done by Jon J. Franczyk (DOGAMI). Gneiss Editing, Portland, OR provided editing services. Critical and insightful reviews by Kate Ely (CTUIR), Mark Ferns (DOGAMI-retired), Joe Kemper (OWRD), Jen Woody (OWRD), Andrew Wentworth (OWRD), and Lalo Guerrero (DOGAMI) greatly enriched the final geologic maps and geodatabase.

REFERENCES

Baksi, A.K., 2022, New ^{40}Ar/^{39}Ar ages from the Grande Ronde and Wanapum Basalt, Columbia River Basalt Group (CRBG): Compilation of all ages and relationship to the geomagnetic polarity time scale for ˜17–15 Ma: Journal of Earth System Science, v. 131 158, p. 1-29. https://www.ias.ac.in/article/fulltext/jess/131/0158, accessed February 17, 2023.

Barry, T.L., Kelley, S.P., Reidel, S.P., Camp, V.E., Self, S., Jarboe, N.A., Duncan, R.A., and Renne, P.R., 2013, Eruption chronology of the Columbia River Basalt Group, *in* Reidel, S.P., Camp, V.E., Martin, M.E., Ross, M.E., Wolff, J.A., Martin, B.S., Tolan, T.L., and Wells, R.E., eds., The Columbia River Flood Basalt Province: Geological Society of America Special Paper 497, p. 45–66. https://pubs.geoscienceworld.org/books/book/661/chapter-abstract/3807104/Eruption-chronology-of-the-Columbia-River-Basalt?redirectedFrom=fulltext, accessed February 17, 2023.

Blakely, R.J., Sherrod, B.L., Weaver, C.S., Wells, R.E., and Rohay, A.C., 2014, The Wallula fault and tectonic framework of south-central Washington, as interpreted from magnetic and gravity anomalies: Tectonophysics, v. 624, p. 32-45. https://www.sciencedirect.com/science/article/abs/pii/S0040195113006501?via%3Dihub, accessed February 17, 2023.

Blakely, R.J., and Sherrod, B.L. and Weaver, C.S., 2020a, High-Resolution Aeromagnetic Survey of the Pasco Area, Washington and Oregon: U.S. Geological Survey data release, https://doi.org/10.5066/P96U1HY0, accessed February 17, 2023.

Blakely, R.J., Sherrod, B.L., Glen, J.M., Ritzinger, B.T., and Mills, P.F., 2020b, High-Resolution Aeromagnetic Survey Over Pendleton, Oregon, and Surrounding Areas: U.S. Geological Survey data release, https://doi.org/10.5066/P9V23JA6, accessed February 17, 2023.

Busacca, A.J., 1989, Long Quaternary record in eastern Washington, U.S.A., interpreted from multiple buried paleosols in loess. Geoderma 45, 105e122. https://www.sciencedirect.com/science/article/abs/pii/0016706189900451, accessed February 17, 2023.

Bush, J. H., Jr.; Morton, J. A.; Anderson, J. V.; Crosby, J. W., III; and Siems, B. A., 1973, Test-observation well near Walla Walla, Washington—Description, stratigraphic relationships and preliminary results: Washington State University College of Engineering Research Division Research Report 73/15-66, 1 v.

Cahoon, E.B., Streck, M.J., Koppers, A.A.P., and Miggins, D.P., 2020, Reshuffling the Columbia River Basalt chronology—Picture Gorge Basalt, the earliest- and longest-erupting formation: Geology, v. 48, p. 348-352. https://doi.org/10.1130/G47122.1, accessed February 17, 2023.

Cohen, K.M., Finney, S.C., Gibbard, P.L. and Fan, J.X., 2013 (updated 2015), The ICS International Chronostratigraphic Chart: Episodes 36, p. 199-204. International Commission on Stratigraphy, accessed February 17, 2023.

Derkey, R.E., Stradling, D.F., Lindsey, K.A., and Tolan, T.L., 2006, Geologic Map of the College Place and Walla Walla 7.5-minute Quadrangles, Walla Walla County, Washington, and Umatilla County, Oregon: Washington Division of Geology and Earth Resources Geologic Map GM-62, 1 plate, scale 1:24,000. https://www.dnr.wa.gov/publications/ger_gm62_geol_map_collegeplace_wallawalla_24k.pdf, accessed February 17, 2023.

Dicken, S.N., 1965, Oregon Geography: The people, the place, and the time, 4th ed: Ann Arbor, Mich., Edwards Brothers, 147 p.

Duda, C.J.M., McClaughry, J.D., Houston, R.A., and Niewendorp, C.A., 2018, Lidar and Structure from Motion-enhanced geologic mapping, examples from Oregon, in Thorleifson, L. H., ed., 2018, Geologic Mapping Forum 2018 Abstracts: Minnesota Geological Survey Open File Report OFR-18-1, 107 p. https://conservancy.umn.edu/handle/11299/194852, accessed February 17, 2023.

Duda, C.J.M., McClaughry, J.D., and Madin, I.P., 2019, Building the modern geologic map in Oregon: a multi-faceted field- and technology-based approach: Geological Society of America Abstracts with Programs. v. 51, no. 4. https://gsa.confex.com/gsa/2019CD/meetingapp.cgi/Paper/329552, accessed February 17, 2023.

Ferns, M.L., 2006a, Preliminary geologic map of the Cayuse 7.5′ quadrangle, Umatilla County, Oregon: Oregon Department of Geology and Mineral Industries Open-File Report O-06-08, 1 plate, scale 1:24,000. https://www.oregongeology.org/pubs/ofr/O-06-08.zip, accessed February 17, 2023.

Ferns, M.L., 2006b, Preliminary geologic map of the Thorn Hollow 7.5′ quadrangle, Umatilla County, Oregon: Oregon Department of Geology and Mineral Industries Open-File Report O-06-10, 1 plate, scale 1:24,000. https://www.oregongeology.org/pubs/ofr/O-06-10.zip, accessed February 17, 2023.

Ferns, M.L., and McClaughry, J.D., 2013, Stratigraphy and volcanic evolution of the middle Miocene La Grande – Owyhee eruptive axis in eastern Oregon, *in* Reidel, S.P., Camp, V. Ross, M.E., Wolff, J.A., Martin, B.E., Tolan, T.L., and Wells, R.E., eds., The Columbia River Flood Basalt Province: Geological Society of America Special Paper 497, p. 401-427, doi:10.1130/2013.2497(16). https://pubs.geoscienceworld.org/books/book/661/chapter-abstract/3807352/Stratigraphy-and-volcanic-evolution-of-the-middle?redirectedFrom=fulltext, accessed February 17, 2023.

Ferns, M.L. and McConnell, V.S., 2006, Preliminary geologic map of the Cabbage Hill 7.5′ quadrangle, Umatilla County, Oregon: Oregon Department of Geology and Mineral Industries Open-File Report O-06-14, 1 plate, scale 1:24,000. https://www.oregongeology.org/pubs/ofr/O-06-14.zip, accessed February 17, 2023.

Ferns, M.L., McConnell, V.S., Madin, I.P., and Johnson, J.A., 2010, Geology of the Upper Grande Ronde River Basin, Union County, Oregon: Oregon Department of Geology and Mineral Industries Bulletin 107, 65 p., 1 pl., scale 1:100,000, Esri™ format shapefiles, dbf files; spreadsheet (5 sheets), geo-located photographs (19). https://www.oregongeology.org/pubs/B/p-B-107.htm, accessed February 17, 2023.

Franczyk, J. J., Madin, I. P., Duda, C. J. M., and McClaughry, J. D., 2020, Oregon geologic data compilation, release 7 [OGDC-7] (statewide): Oregon Department of Geology and Mineral Industries Digital Data Series OGDC-7, Esri geodatabase. https://www.oregongeology.org/pubs/dds/p-OGDC-7.htm, accessed February 17, 2023.

Geological Society of America Rock-Color Chart Committee, 1991, Rock color chart, 7th printing: Boulder, CO.

Gradstein, F.M., Ogg, J.A., and Smith, A., G., 2004, A Geologic Time Scale 2004, Cambridge University Press, 589 p.

Hogenson, G.M., 1964, Geology and ground water of the Umatilla River basin, Oregon: U.S. Geological Survey Water Supply Paper 1620, 162 p. https://pubs.er.usgs.gov/publication/wsp1620, accessed February 17, 2023.

Hooper, P.R., 2000, Chemical discrimination of Columbia River Basalt flows: Geochemistry, Geophysics, and Geosystems, v. 1, no. 1, p. 1-14. https://onlinelibrary.wiley.com/doi/10.1029/2000GC000040/pdf, accessed February 17, 2023.

Hooper, P.R., and Conrey, R.M., 1989, A model for the tectonic setting of the Columbia River basalt eruptions, *in* Reidel, S.P., and Hooper, P.R., eds., Volcanism and tectonism in the Columbia River flood-basalt province: Boulder, Colorado, Geological Society of America Special Paper 239, p. 293-306. https://pubs.geoscienceworld.org/gsa/books/book/375/chapter-abstract/3797047/A-model-for-the-tectonic-setting-of-the-Columbia?redirectedFrom=fulltext accessed February 17, 2023.

Hutter, I. L., 1997, The Wallula Fault Zone: A study of the structure and tectonic history of a portion of the Olympic-Wallowa Lineament: Bellingham, Western Washington University, M.S. Thesis, 194 p.

Johnson, D.M., Hooper, P.R., and Conrey, R.M., 1999, XRF analysis of rocks and minerals for major and trace elements on a single low dilution Li-tetraborate fused bead: Advances in X-ray Analysis, v. 41, p. 843-867. XRF Method | School of the Environment | Washington State University (wsu.edu), accessed February 17, 2023.

Johnson, D.R., and Makinson, A.J., 1988, Soil survey of Umatilla County Area, Oregon: Natural Resources Conservation Service Soil Conservation Survey 667, 388 p. https://nrcs.app.box.com/s/taycqfsrlbxjocs6ck4a68y96gqsvd76/file/982604665170, accessed February 17, 2023.

Kasbohm, J., and Schoene, B., 2018, Rapid eruption of the Columbia River flood basalt and correlation with mid-Miocene climate optimum; Science Advances, v. 4, no. 9. https://advances.sciencemag.org/content/4/9/eaat8223, accessed February 17, 2023.

Kendal, J.J., 1981, The geology and structure of the Blue Mountains in northeastern Umatilla County, Oregon: Los Angeles, University of Southern California, M.S. Thesis, 103 p.

Kienle, C.F., Jr., Hamill, M.L., and Clayton, D.N., 1979, Geological Reconnaissance of the Wallula Gap Washington - Blue Mountains - La Grande, Oregon region: Unpublished report prepared for the Washington Public Power Supply System by Shannon and Wilson Inc., contract o. 44013, C.O. No 38, 58 p.

Kuehn, S. C., 1995, The Olympic-Wallowa Lineament, Hite Fault System, and Columbia River Basalt Group Stratigraphy in northeast Umatilla County, Oregon: Pullman, Washington State University, M.S. Thesis, 170 p.

Laval, W.N., 1956, Stratigraphy and Structural Geology of Portions of South-Central Washington: Ph.D. dissertation, Seattle, University of Washington, 208 p.

Le Maitre, R.W. (ed.), and others, 2004, Igneous rocks: A classification and glossary of terms: Cambridge University Press, Recommendations of the International Union of Geological Sciences, Subcommission on the Systematics of Igneous Rocks, 236 p.

Lewis, P.F., 1960, Linear topography in the southwestern Palouse, Washington-Oregon: Annals of the Association of American Geographers, v. 50, no. 2, p. 98-111.

Mackenzie, W.S., Donaldson, C.H., and Guilford, C., 1997, Atlas of igneous rocks and their textures: Addison Wesley Longman Ltd., 7th ed., 148 p.

Madin, I.P., and Geitgey, R.P., 2007, Preliminary geologic map of the Umatilla Basin, Morrow and Umatilla Counties, Oregon: Oregon Department of Geology and Mineral Industries Open-File Report O-07-15, 3 plates, scale 1:100,000. https://www.oregongeology.org/pubs/ofr/O-07-15.zip, accessed February 17, 2023.

Madin, I.P., McClaughry, J.D., and Azzopardi, C.J.M., 2023, Geologic map of the Milton Freewater and Bowlus Hill 7.5′ quadrangles: Oregon Department of Geology and Mineral Industries Geological Map Series GMS 130, 3 plates, scale 1:24,000, Esri format geodatabase; shapefiles, metadata; spreadsheets (16 sheets). https://www.oregongeology.org/pubs/gms/gms-130/gms-130.htm, accessed February 17, 2023.

Mahood, G.A., and Benson, T.R., 2017, Using ^{40}Ar ^{39}Ar ages of intercalated silicic tuffs to date flood basalts: Precise ages for Steens Basalt Member of the Columbia River Basalt Group: Earth and Planetary Science Letters, v. 459, p. 340-351. https://www.sciencedirect.com/science/article/abs/pii/S0012821X16306720?via%3Dihub, accessed February 17, 2023.

McDonald, E.V., and Busacca, A.J., 1988, Record of pre-late Wisconsin giant floods in the Channeled Scabland interpreted from loess deposits: Geology, v. 16, no. 8, p. 728-731 https://pubs.geoscienceworld.org/gsa/geology/article-abstract/16/8/728/204738/Record-of-pre-late-Wisconsin-giant-floods-in-the, accessed February 17, 2023.

McDonald, E.V., Sweeney, M.R., and Busacca, A.J., 2012, Glacial outburst floods and loess sedimentation documented during Oxygen Isotope Stage 4 on the Columbia Plateau, Washington State: Quaternary Science Reviews v. 45, p. 18-30. https://www.sciencedirect.com/science/article/abs/pii/S0277379112001412, accessed February 17, 2023.

Moore, N.E., Grunder, A.L., and Bohrson, W.A., 2018, The three-stage petrochemical evolution of the Steens Basalt (southeast Oregon, USA) compared to large igneous provinces and layered mafic intrusions: Geosphere, v. 14, p. 2505-2532. https://pubs.geoscienceworld.org/gsa/geosphere/article/14/6/2505/548601/The-three-stage-petrochemical-evolution-of-the, accessed February 17, 2023.

Newcomb, R.C., 1965, Geology and groundwater resources of the Walla Walla River basin, Washington-Oregon: Washington Division of Water Resources Water Supply Bulletin 21, 151 p. https://apps.ecology.wa.gov/publications/summarypages/wsb21.html, accessed February 17, 2023.

Ogg, J.G., Ogg, G., and Gradstein, F.M., 2008, Concise geologic time scale. Cambridge, University Press, 177.

Personius, S.F., Dart, R.L., Bradley, L.A., and Haller, K.M., 1995, Map and data for Quaternary faults and folds in Oregon: U.S. Geological Survey Open-File Report 03-095, 556 p. https://pubs.usgs.gov/of/2003/ofr-03-095/OFR_03_095_text.pdf, accessed February 17, 2023.

Piersol, M.W., and Sprenke, K.F., 2015, A Columbia River Basalt Group Aquifer in sustained drought: Insight from Geophysical Methods: Resources, v. 4., p. 557-596. https://www.mdpi.com/2079-9276/4/3/577, accessed February 17, 2023.

Raisz, E., 1945, The Olympic-Wallowa Lineament: American Journal of Science, v. 243-A, p. 479-485.

Reidel, S.P., and Tolan, T.L., 2013, The Grande Ronde Basalt, Columbia River Basalt Group, *in* Reidel, S.P., Camp, V.E., Martin, M.E., Ross, M.E., Wolff, J.A., Martin, B.S., Tolan, T.L., and Wells, R.E., eds., The Columbia River Flood Basalt Province: Boulder, Colorado, Geological Society of America Special Paper 497, p. 117-154. https://pubs.geoscienceworld.org/books/book/661/chapter-abstract/3807152/The-Grande-Ronde-Basalt-Columbia-River-Basalt?redirectedFrom=fulltext, accessed February 17, 2023.

Reidel, S.P., Johnson, V.G., and Spane, F.A., 2002, Natural gas storage in basalt aquifers of the Columbia Laboratory, Basin, Pacific Northwest USA: a guide to site characterization: Richland, Wash., Pacific Northwest National 277 p. https://www.pnnl.gov/main/publications/external/technical_reports/PNNL-13962.pdf, accessed February 17, 2023.

Reidel, S.P., Campbell, N.P., Fecht, K.R., and Lindsey, K.A., 1994, Late Cenozoic structure and stratigraphy of south-central Washington, *in* Lasmanis, R., and Cheney, E.S., eds., Regional geology of Washington State: Washington Division of Geology and Earth Resources, p. 159-180.

Reidel, S.P., Camp, V.E., Tolan, T,L., and Martin, B.S., 2013a, The Columbia River flood basalt province: Stratigraphy, aerial extent, volume, and physical volcanology, *in* Reidel, S.P., Camp, V.E., Martin, M.E., Ross, M.E., Wolff, J.A., Martin, B.S., Tolan, T.L., and Wells, R.E., eds., The Columbia River Flood Basalt Province: Boulder, Colorado, Geological Society of America Special Paper 497, p. 1-43. https://pubs.geoscienceworld.org/books/book/661/chapter-abstract/3807083/The-Columbia-River-flood-basalt-province?redirectedFrom=fulltext, accessed February 17, 2023.

Reidel, S.P., Camp, V.E., Tolan, T.L., Kauffman, J.D., and Garwood, D.L., 2013b, Tectonic evolution of the Columbia River flood basalt province, in Reidel, S.P., Camp, V.E., Martin, M.E., Ross, M.E., Wolff, J.A., Martin, B.S., Tolan, T.L., and Wells, R.E., eds., The Columbia River Flood Basalt Province: Boulder, Colorado, Geological Society of America Special Paper 497, p. 293-324. https://pubs.geoscienceworld.org/books/book/661/chapter-abstract/3807278/Tectonic-evolution-of-the-Columbia-River-flood?redirectedFrom=fulltext, accessed February 17, 2023.

Reidel, S.P., Fecht, K.R., Hutter (Harrold) I.L., Tolan, T., and Chamness, M.A., 2021, The Olympic-Wallowa lineament: A new look at an old controversy: Geological Society of America Bulletin, v. 133, p. 115-133. https://pubs.geoscienceworld.org/gsa/gsabulletin/article-abstract/133/12/115/586095/The-Olympic-Wallowa-lineament-A-new-look-at-an-old?redirectedFrom=fulltext, accessed February 17, 2023.

Riddihough, R., Finn, C., and Couch, R., 1986, Klamath–Blue Mountain lineament, Oregon: Geology, v. 14, p. 528–531. https://pubs.geoscienceworld.org/gsa/geology/article abstract/14/6/528/204089/Klamath-Blue-Mountain-lineament-Oregon, accessed February 17, 2023.

Seims, B.A., Bush, J.G., and Crosby, J.W. III, 1974, TiO_2 and geophysical logging criteria for Yakima Basalt correlation, Columbia Plateau: Geological Society of America Bulletin, v. 85, 1061-1068. https://pubs.geoscienceworld.org/gsa/gsabulletin/article-abstract/85/7/1061/201633/TiO2-and-Geophysical-Logging-Criteria-for-Yakima, accessed February 17, 2023.

Sherrod, B.L., Blakely, R.J., Lasher, J.P., Lamb, A., Mahan, S.A., Foit, F.F., Jr., and Barnett, E.A., 2016, Active faulting on the Wallula fault zone within the Olympic-Wallowa lineament, Washington State, USA: Geological Society of America Bulletin, v. 128, p. 1639-1659. https://pubs.geoscienceworld.org/gsa/gsabulletin/article/128/11-12/1636/185319/Active-faulting-on-the-Wallula-fault-zone-within, accessed February 17, 2023.

Staisch, L.M., Angster, S., Bennett, S.E.K., Blakely, R,J., Sherrod, B., Stephenson, W., and Lasher, J., 2022, Geomorphology, geophysics, and geology along the Wallula fault zone, Washington and Oregon: Geological Society of America Abstracts with Programs. Vol 54, No. 5. https://gsa.confex.com/gsa/2022AM/webprogram/Paper381799.html, accessed February 17, 2023.

Swanson, D.A., Wright, T.L., Hooper, P.R., and Bentley, R.D., 1979, Revisions in stratigraphic nomenclature of the Columbia River Basalt Group: U.S. Geological Survey Bulletin 1457-G, 59 p., 1 pl. https://pubs.er.usgs.gov/publication/b1457G, accessed February 17, 2023.

Swanson, D.A., Anderson, J.L., Camp, V.E., Hooper, P.R., and Taubeneck, W.H., 1981, Reconnaissance geologic map of the Columbia River Basalt Group, northern Oregon and western Idaho: U.S Geological Survey Open-File Report OF-81-797, 5 plates, 1:250,000. https://pubs.er.usgs.gov/publication/ofr81797, accessed February 17, 2023.

Tolan, T.L., and Reidel, S.P., 1989, Structure map of a portion of the Columbia River flood-basalt Province, *in* Reidel, S.P., and Hooper, P.R., eds., Volcanism and tectonism in the Columbia River Flood-Basalt Province: Geological Society of America Special Paper 239, 1 sheet, scale 1:500,000.

Tolan, T.L., Martin, B.S., Reidel, S.P., Anderson, J.L., Lindsey, K.A., and Burt, W., 2009, An introduction to the stratigraphy, structural geology, and hydrogeology of the Columbia River flood-basalt province: A primer for the GSA CRBG field trips, *in* O'Connor, J. E., Dorsey, R. J., and Madin, I. P., eds., Volcanoes to Vineyards: geologic field trips through the dynamic landscape of the Pacific Northwest: Geological Society of America Field Guide 15, p. 599-643. https://pubs.geoscienceworld.org/books/book/885/chapter-abstract/3931355/An-introduction-to-the-stratigraphy-structural?redirectedFrom=fulltext, accessed February 17, 2023.

U.S. Energy Research and Development Administration, 1976, Preliminary Feasibility Study on Storage of Radioactive Waste in Columbia River Basalts: U.S. Energy Research and Engineering Division Report ARH-ST-137 under contract E(45-1)-2130, 183 p.

U.S. Geological Survey National Cooperative Geologic Mapping Program, 2020, GeMS (Geologic Map Schema)—A standard format for the digital publication of geologic maps: U.S. Geological Survey Techniques and Methods, book 11, chap. B10, 74 p. https://doi.org//10.3133/tm11B10, accessed February 17, 2023.

Walker, G. W., 1973, Reconnaissance geologic map of the Pendleton quadrangle, Oregon and Washington: U.S. Geological Survey Miscellaneous Geologic Investigations Map I-727, scale 1:250,000. https://pubs.er.usgs.gov/publication/i727, accessed February 17, 2023.

Washington Geological Survey, Geologic provinces of Washington. https://www.dnr.wa.gov/programs-and-services/geology/explore-popular-geology/geologic-provinces-washington, accessed February 17, 2023.

Wetzel, K.F., Bennett, S.E.K., Staisch, L., Blakely, R.J., Lamb, A.P., and Earney, T., 2018, Field geophysical investigations of the Blue Mountains uplift, northeastern Oregon: American Geophysical Union, Fall Meeting 2018, abstract #T51G-0250. Field geophysical investigations of the Blue Mountains uplift, northeastern Oregon - NASA/ADS (harvard.edu), accessed February 17, 2023.

Figure 1. Map of some major volcanic and structural features in Oregon. The extent of the Walla Walla River basin is shown by a light blue line. The Athena 7.5′ quadrangle is shown by a red polygon in northeastern Oregon. The light brown area is the outcrop distribution of the CRBG, including areas from which the lava flows have been eroded, in addition to areas where lava flows are concealed by younger units. Red dashed lines show the area of dike swarms from which CRBG lava flows were erupted (CJD – Chief Joseph Dike Swarm; PDG – Picture Gorge Dike Swarm; SD – Steens Dike Swarm). Modified from Reidel and others (2013) and Ferns and McClaughry (2013). Labels: BG – Baker graben; BV – Boring Volcanic Field; HFS – Hite fault zone; HRF – Hood River fault zone; HCF – Horse Creek fault zone; GCF – Gales Creek fault; GRF – Green Ridge fault zone; LG – La Grande graben; OIG – Oregon-Idaho graben; PB – Portland Basin; PHF – Portland Hills fault; MHFZ – Mount Hood fault zone; SV – Simcoe Mountains; SR – Steens Mountain; TB – Tualatin Basin; WFZ – Wallula fault zone. Oregon physiographic provinces after Dicken (1965). Geologic provinces of Washington from the Washington Geological Survey.

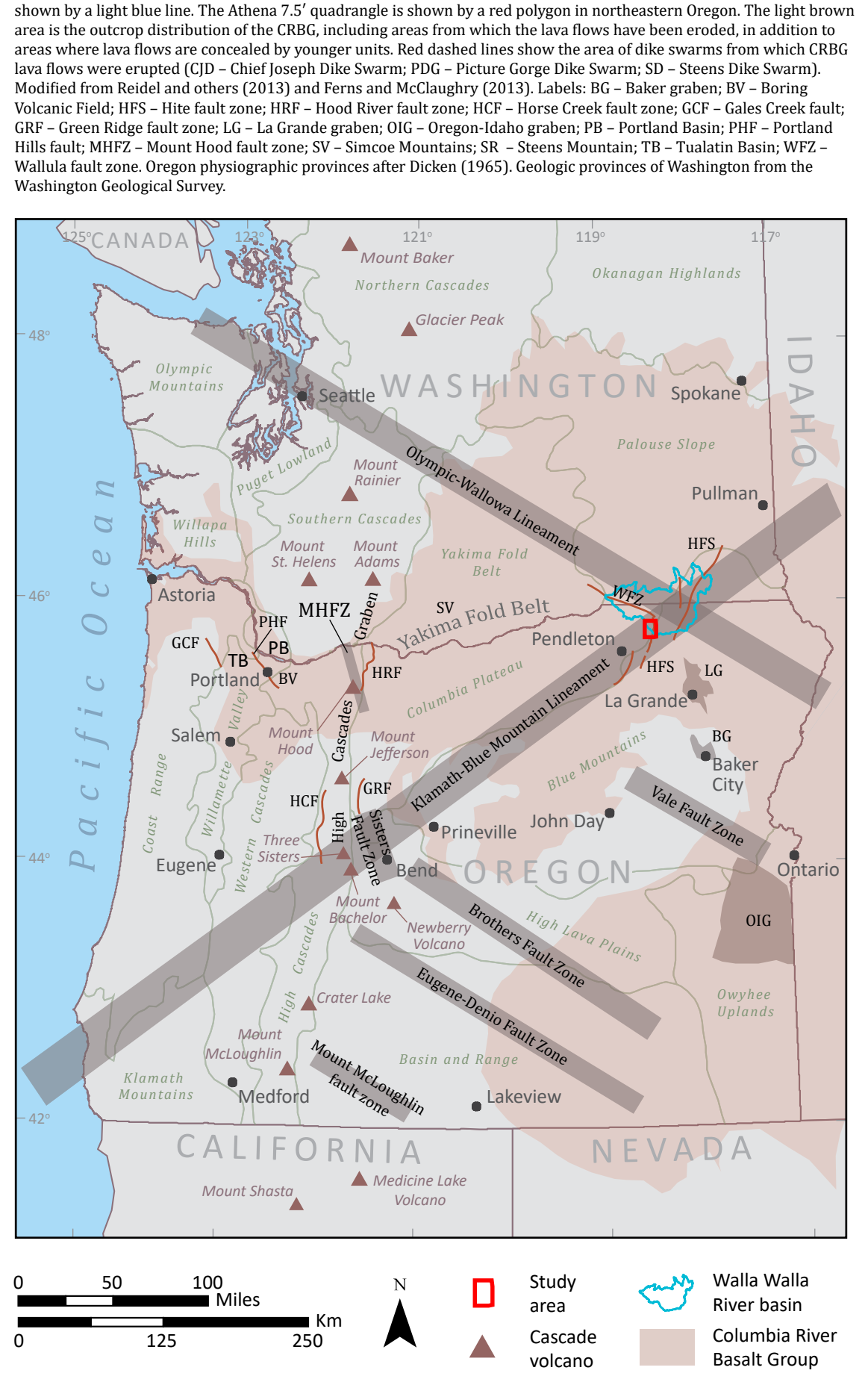

Figure 2. Chart showing the lava flow stratigraphy of the CRBG. Modified from Reidel and others (2002), with updated stratigraphy from Reidel and others (2013a) and Reidel and Tolan (2013a). U-Pb ages from Kasbohm and Schoene (2018) are shown in parentheses, for example (15.895). ^{40}Ar/^{39}Ar ages from Mahood and Benson (2017) are shown in square brackets, for example [16.54]. Selected ^{40}Ar/^{39}Ar ages for the Picture Gorge Basalt from Cahoon and others (2020) are shown in curly brackets, for example {16.22}. Age of the base of Steens Basalt from Moore and others (2018) is shown in vertical brackets, for example |16.97|.

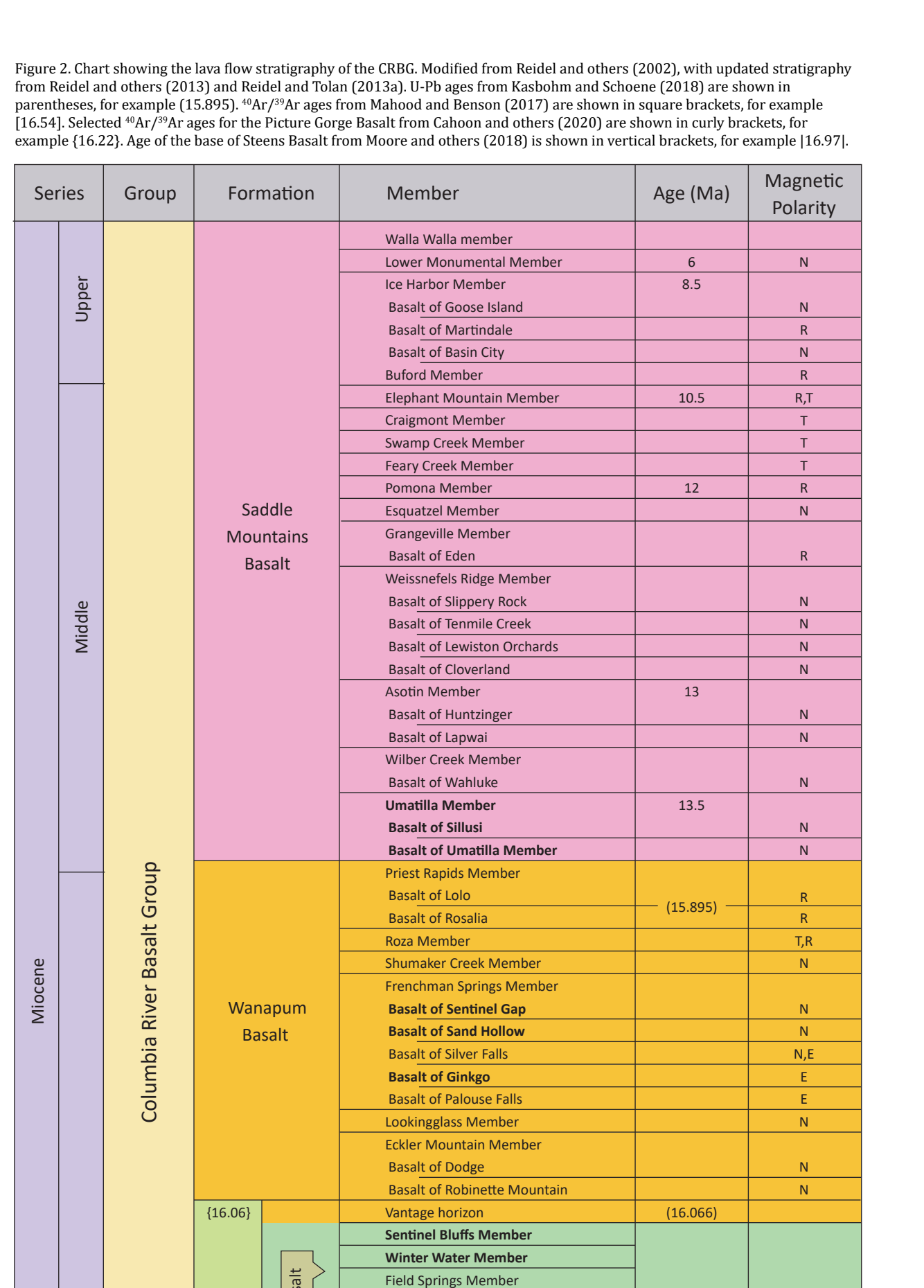

Figure 3. Structure maps of Athena and the surrounding area, showing faults, folds, and high-resolution aeromagnetic data. (A) Mapped faults and folds drawn across a USGS 10-m DEM. (B) Total-field high-resolution aeromagnetic anomaly map (Blakely and others, 2020a, b). The map in B shows a partially transparent classified color ramp of the magnetic data area overlain across a hillshade applied to the magnetic data. Mapped faults and folds shown are from this publication, Madin and others (2023), and Franczyk and others (2020).

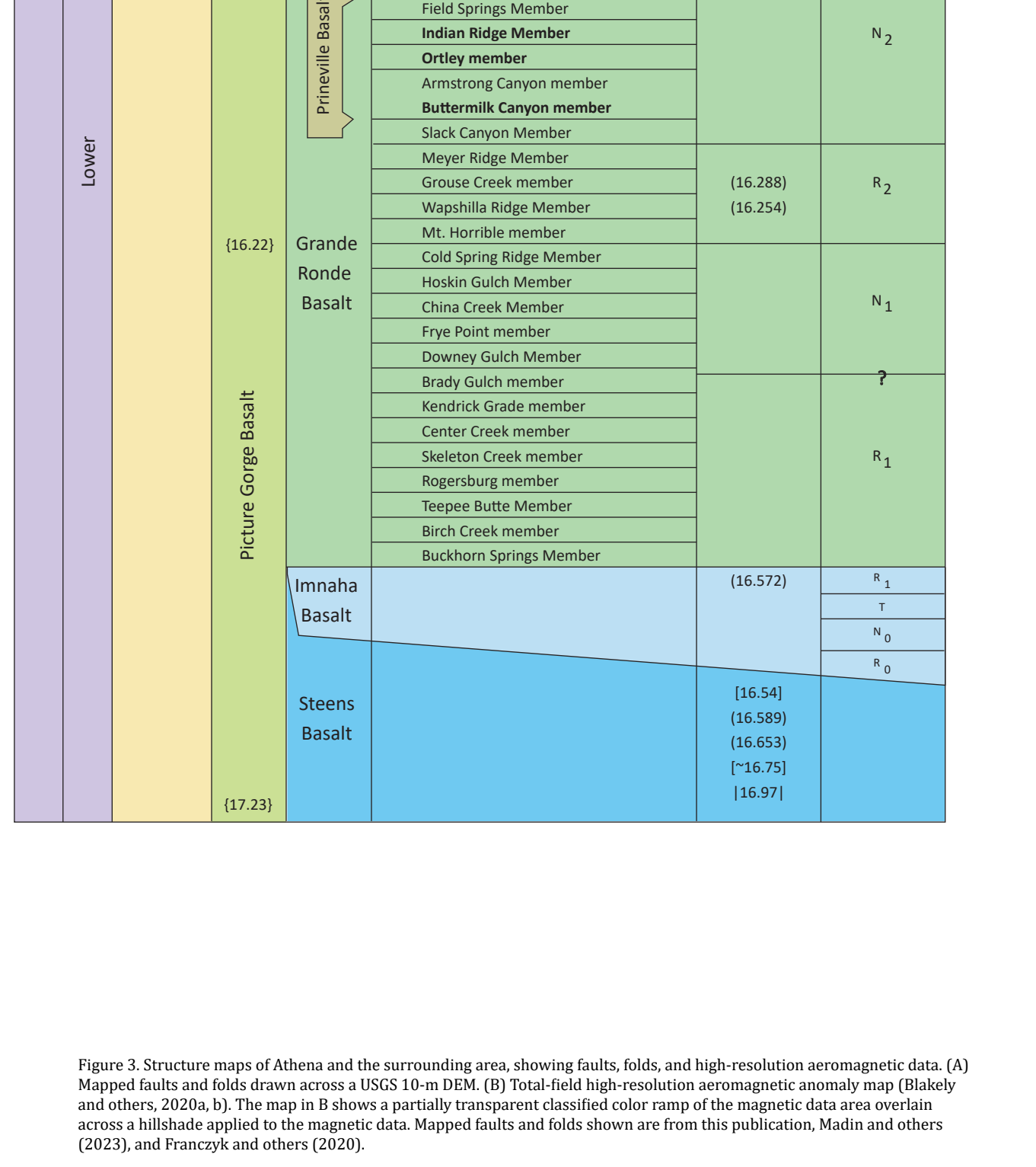

Figure 4. Trace of the Dry Creek fault exposed in a roadcut along OR Highway 11, near the confluence of Little Dry Creek and Dry Creek. The Dry Creek fault is a N.1°E., 56°NW.-oriented, down-on-the-northwest normal fault displacing high-phosphorus lava flows of the Basalt of Sentinel Gap (**Twfsh**). Conglomerate (**QTcg**) and loess (**Qlo**) lie across, but are not broken by the fault.

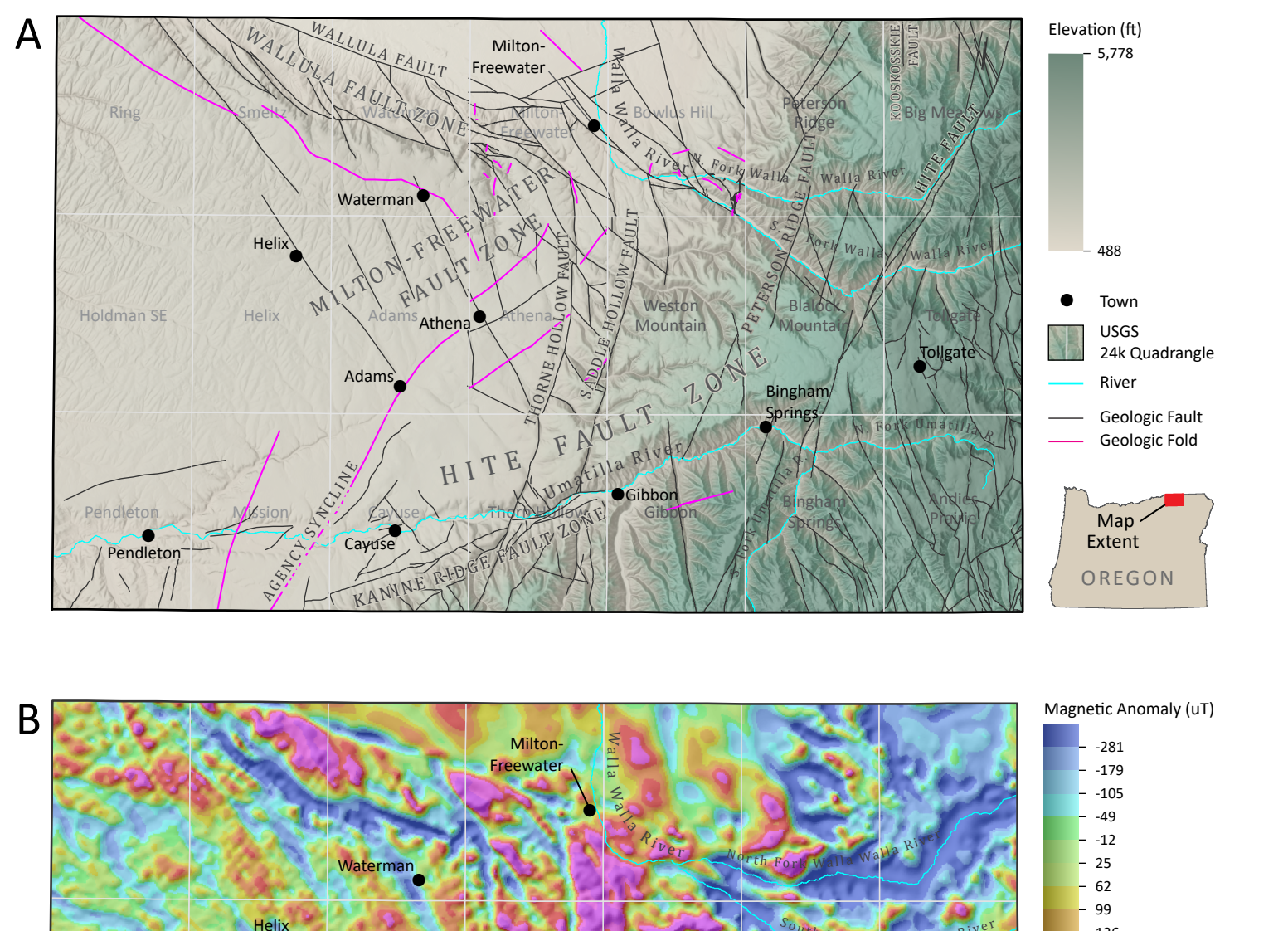

EXPLANATION OF MAP UNITS

UPPER CENOZOIC SURFICIAL DEPOSITS

Qf **modern fill and construction material (upper Holocene)** — Uncompacted to engineered and reinforced artificial or constructed deposits of poorly sorted and crudely layered mixed gravel, sand, clay, and other engineered fill (Plate 1). Areas mapped as **Qf** in the map area are generally associated with road embankments, dams and levees, culvert fills, and mined land (Plate 1). Older fills are likely uncompacted versus newer fills, which are likely engineered and reinforced using geotextiles or retaining structures. The thickness of fill deposits is as much as 30 m. Unit **Qf** is assigned a late Holocene age, ranging in age from the late 1800s to recent times.

Qa **alluvium (Holocene and Upper Pleistocene)** — Unconsolidated, poorly- to moderately-stratified gravel, sand, silt, and clay mapped in and adjacent to stream channels and on associated floodplains (Plate 1). Thickness of unit **Qa** is generally < 5 to 7 m; bedrock units may be locally exposed in the base of stream channels within areas mapped as unit **Qa**. Unit **Qa** is assigned a Late Pleistocene and Holocene age. Areas mapped as **Qa** may include deposits containing human-made debris or artifacts, or deposits filling areas known to have been modified by humans such as excavations, roadways, or gravel pits.

Qaf **fan deposits (Holocene and Upper Pleistocene)** — Unconsolidated, poorly sorted, poorly graded deposits of boulders, cobbles, pebbles, granules, sand, silt, and clay in fan-shaped accumulations at the mouths of small and steep drainages (Plate 1). The local thickness of alluvial fan deposits (**Qaf**) is variable but is probably <15 m. Unit **Qaf** includes fan deposits of Late Pleistocene and Holocene age.

Qlo **loess deposits (Holocene to lower Pleistocene)** — Chiefly pale yellowish brown (10YR 6/2), micaceous, quartzo-feldspathic silt with very fine-grained sand and clay mantling the CRBG in the western part of the Athena 7.5′ quadrangle (Plate 1; Figure 3a). Thinner loess deposits (**Qlo**) discontinuously cover the CRBG in highlands along the eastern side of the map area (Plate 1). Loess (**Qlo**) typically forms a massive, featureless deposit that has been extensively modified by dry-land agriculture over the past century. Where the antecedent deposit was originally thin or has been further thinned by deep agricultural tilling, silt may be mixed with larger rock fragments from the underlying bedrock geology. Commonly, the edges of fields constructed in loess (**Qlo**), are characterized by steep 1- to 2-m-high embankments created from circular, annual tilling of large fields. Thickness of unit **Qlo** ranges from thin veneers <1 m to as much as 20 m, on the basis of information reported from well logs; roadcuts may locally show up to 6 m of loess (**Qlo**) in vertical section.

The distribution of loess (**Qlo**) is mapped here on the basis of field observations, soil mapping by Johnson and Makinson (1988), geologic mapping by Swanson and others (1981) and Madin and Geitgey (2007), and interpretation of the 2020 NAIP orthophoto of Umatilla County (Plate 1). Most of the contacts represent human-modified boundaries. Thin loess (**Qlo**) deposits of limited distribution have not been mapped where the underlying geology can be reasonably inferred or is known to be present at the surface.

Loess (**Qlo**) mapped in the Athena 7.5′ quadrangle is part of a more extensive unit of wind-laid silt covering >50,000 km² on the Columbia Plateau in southeastern Washington, western Idaho, and northeastern Oregon (Figure 1; Figure 3a). In northeastern Oregon, the area of **Qlo** has a pronounced N30°E-trending linear topographic grain, expressed by linear ridges and the parallel orientation of minor drainages (Figure 3a; Lewis, 1960; Madin and Geitgey, 2007). Loess (**Qlo**) in the Athena 7.5′ quadrangle is assigned an early Pleistocene to Holocene age on the basis of presumed correlation with well-studied **Qlo** mantling the CRBG across the Palouse of southeastern Washington (Figures 1 and 3a; McDonald and others, 2012). McDonald and others (2012) describe three loess sequences (L1, L2, L3) in the Palouse dating back ~70,000 years; normal-reversed-normal polarity signatures suggest that older loess in the region may date back to 1 to 2 Ma (McDonald and Busacca, 1988; Busacca, 1989).

Unconformity

UPPER CENOZOIC VOLCANIC AND SEDIMENTARY ROCKS

QTcg **conglomerate (lower Pleistocene[?], Pliocene[?], or upper Miocene)** — Chiefly unconsolidated to poorly consolidated conglomerate composed entirely of well-rounded clasts of basaltic composition, contained within a silicic to calcic, muddy to sandy matrix. The unit is mapped above the CRBG (**Twfsl**) in a northeast-trending belt between the city of Athena and the northeast corner of the Athena 7.5′ quadrangle (Plate 1; Figure 3a). The conglomerate (**QTcg**) is largely buried beneath extensive loess (**Qlo**) deposits, cropping out only above the Basalt of Sentinel Gap (**Twfsl**) along OR Highway 204 north of Weston, in a roadcut exposing the Dry Creek fault along OR Highway 11 near the confluence of Little Dry Creek and Dry Creek (Plate 1; Figure 4), and above the Basalt of Sand Hollow (**Twfh**) along Blue Mountain Station Road, 0.4 km east of the northeast corner of the Athena 7.5′ quadrangle (Figure 3a). Lithologic descriptions of cemented gravel from two water wells (e.g., UMAT 3074, UMAT 3082) and anomalous rounded hill topography recognized in lidar DEMs suggest the presence of the unit **QTcg** in the subsurface beneath loess (**Qlo**) and above the CRBG near Weston (Plate 1).

Conglomerate (**QTcg**) mapped at Weston is interpreted to correlate with cemented sandy conglomerate interbedded with layers of sandstone and claystone recognized in boreholes drilled in the Walla Walla Valley (Madin and others, 2023; Figure 3a). The conglomerate (**QTcg**) also crops out in a few highland areas directly adjacent to the main part of the Walla Walla Valley (Derkey and others, 2006; Madin and others, 2023). The age range of unit **QTcg** in the Athena 7.5′ quadrangle and Walla Walla Valley is uncertain (Figure 3a). In both areas the unit generally lies directly above middle to upper Miocene CRBG lava flows and below alluvium (**Qa**), Missoula Flood deposits, and loess (**Qlo**). Conglomerate (**QTcg**) was deposited by the ancestral Walla Walla River and tributaries in the Walla Walla River basin. Unit **QTcg** is assigned a late Miocene, Pliocene(?), or to early Pleistocene(?) age on the basis of stratigraphic position.

Disconformity

COLUMBIA RIVER BASALT GROUP

The CRBG is an extensive succession of tholeiitic basalt and basaltic andesite lava flows covering more than 210,000 km² in parts of Washington, Oregon, Idaho, and Nevada (Figures 1 and 2; Reidel and others, 2013a). Lava flows assigned to the Saddle Mountains, Wanapum, and Grande Ronde Basalt crop out or are present in the subsurface in the Athena 7.5′ quadrangle (Figures 2 and 3a; Plate 1). CRBG lava flows in the map area are typically characterized by stacked flow lobes, cored by laterally discontinuous blocky- to columnar-jointed basalt, separated by flow tops and bottoms. Where preserved, flow tops may be several meters thick, consisting of hummocky, layered, fine grained crystalline to glassy upper crust with pāhoehoe textures, vesicle-rich scoria, flow breccia, and rubbly pahoehoe (e.g., unit **Twfsl** roadcut north of Dry Creek on OR Highway 11). Flow bottoms are typically thin (<1 m) layers of vesiculated fine grained crystalline to glassy basalt and basal flow breccia; vesicle pipes, pillow-palagonite complexes, and hyaloclastite may be present at the base of lava flows. CRBG units commonly form distinctive bench and slope topography, resulting from differential erosion within and between lava flows. More easily erodible interflow zones are often marked by bands of trees, while more resistant flow interiors typically form continuous cliffs with grass-topped benches. Lava flows weather to shades of brownish gray, brown, and bright orangish-brown. Coarser-grained lava flows commonly weather to form slopes mantled by a mixture of spheroidal weathering core stones and coarse-grained, angular sand grains. Aggregate thickness of the CRBG in the Athena 7.5′ quadrangle may exceed 900 m.

Saddle Mountains Basalt

The Saddle Mountains Basalt, erupted between ~14 and 6 Ma, represents the longest eruptive period of all CRBG formations (Figure 2). The Saddle Mountains Basalt is represented in the map area by the Umatilla Member. Regionally, Saddle Mountains lava flows are confined by paleotopography and form thick, channelized or dammed lava flows characterized by well-developed columnar jointing.

Umatilla Member

Tsu **Umatilla Member (middle Miocene)** — High-titanium and iron-rich basaltic trachyandesite to trachyandesite lava flows (SiO_2 = 53.1 to 55.72 weight percent; TiO_2 = 2.6 to 3.44 weight percent; n = 7 analyses) characterized by high potassium (K_2O = 2.48 to 2.88 weight percent), phosphorus (P_2O_5 = 0.79 to 1.04 weight percent), and barium (Ba = 2791 to 3643 ppm; Figure 5; Tables 1 and 2). Regionally, the Umatilla Member is made up of two chemically distinctive lava flows including the older Basalt of Umatilla and the younger Basalt of Sillusi (Figure 2; Laval, 1956; Reidel and others, 2013). Both are present in the map area. In the Athena 7.5′ quadrangle, the Umatilla Member (**Tsu**) is largely mapped discontinuously capping plateaus, north of the Weston fault (Plate 1; Figure 3a). The unit also crops out near Spring Hollow and tops upland areas at Reed and Hawley Mountain in the southeastern part of the Athena 7.5′ quadrangle (Plate 1; Figure 3a). The Umatilla Member (**Tsu**) often weathers to large blocks that readily form talus slopes. Based on well logs the lava flows are underlain in places by tuffaceous sedimentary rocks. Thickness of unit **Tsu** ranges between 10 and 45 m in the Athena 7.5′ quadrangle; the unit is ~40 m thick in water well UMAT 57710 at Athena (Plate 1; cross section A-A′, Plate 1; Figure 3a). Typical hand samples are medium gray (N5) to medium bluish gray (5B 5/1) and aphyric to very sparsely porphyritic with rare plagioclase and olivine phenocrysts <2 millimeters (mm), distributed in a fine- to very fine-grained holocrystalline groundmass. Both the Basalt of Sillusi and the Basalt of Umatilla have normal magnetic polarity (Figure 2). The Umatilla Member (**Tsu**) is assigned a middle Miocene age on the basis of stratigraphic position and isotopic ages. A K-Ar age of 14.57 was reported for the Umatilla Member by the U.S. Energy Research and Development Administration (1976; recalculated by Barry and others, 2013) while an ^{40}Ar/^{36}Ar – ^{40}Ar/^{39}Ar isochron age of 13.64 + 0.17 Ma was obtained by Ferns and others (2010) in the upper Grande Ronde River basin.

Disconformity

Wanapum Basalt

The Wanapum Basalt in the Athena 7.5′ quadrangle consists of lava flows assigned to the Frenchman Springs Member (Figure 2). Wanapum Basalt lava flows are distinguished in the map area by the presence of widely scattered to conspicuous large plagioclase phenocrysts and markedly higher titanium contents with respect to the older Grande Ronde Basalt (Tables 1 and 2; Figure 5). The age of the Wanapum Basalt ranges between ~16.1 and 15.9 Ma bracketed by U-Pb dates of 15.895 ± 0.019 Ma for ash between the Basalt of Rosalia and Basalt of Lolo (Priest Rapids Member) and 16.066 ± 0.040 Ma for ash from the Vantage Horizon between the Basalt of Ginkgo (**Twfg**) (Frenchman Springs Member) and the Sentinel Bluffs Member (**Tgsmu**) of the older Grande Ronde Basalt (Figure 2; Kasbohm and Schoene, 2018). The Wanapum Basalt is subdivided in the map area into the following units:

Frenchman Springs Member

Basalt of Sentinel Gap (middle or lower Miocene) — Flow-on-flow sequence of high-titanium and iron-rich basalt lava flows (SiO_2 = 51.28 to 53.22 weight percent; TiO_2 = 2.9 to 3.33 weight percent; P_2O_5 = 0.58 to 0.72 weight percent; n = 34 analyses) mapped widely west of the Thorn Hollow fault in the Athena 7.5′ quadrangle (Plate 1; Figures 3a and 5; Tables 1 and 2). These lava flows (**Twfsl**, **Twfsh**) are also mapped discontinuously in uplands between the Thorn Hollow and Saddle Hollow faults in the eastern part of the Athena 7.5′ quadrangle (Plate 1; Figure 3a). The Basalt of Sentinel Gap (**Twfsl**, **Twfsh**) is distinguished from the underlying Basalt of Sand Hollow (**Twfh**) on the basis of relatively higher amounts of titanium (avg TiO_2 = 3.1 weight percent) and phosphorus (avg. P_2O_5 = 0.63 weight percent) and lesser amounts of chromium (avg. Cr = 15 ppm)(Figures 2 and 5; Tables 1 and 2). Thickness of the Basalt of Sentinel Gap (**Twfsl**, **Twfsh**) in the map area is as much as 130 m (Plate 1, cross section A-A′). Typical hand samples of the basalt are medium dark gray (N4) to dark gray (N2) and aphyric to very sparsely porphyritic, with <1 percent (vol.) clear to pale yellowish orange (10YR 8/6) plagioclase microphenocrysts and phenocrysts ≤7 mm and <2 percent (vol.) grayish black (N2) clinopyroxene microphenocrysts ≤1 mm, enclosed within a fine-grained holocrystalline to hypocrystalline groundmass of plagioclase, intergranular clinopyroxene, iron-titanium oxides, and intersertal glass. The Basalt of Sentinel Gap (**Twfsl**, **Twfsh**) has normal magnetic polarity and an early to middle Miocene age between 16.1 and 15.9 Ma (Figure 2). N- to NE-striking dikes correlated with both units of the Basalt of Sentinel Gap have been mapped between the Thorn Hollow and Saddle Hollow faults in the Athena 7.5′ quadrangle (**Twfsl**, **Twfsh**; SiO_2 = 51.48 to 52.92 weight percent; TiO_2 = 3.01 to 3.1 weight percent; P_2O_5 = 0.59 to 0.68 weight percent; Cr = 14 to 19 ppm; n = 3 analyses; Plate 1, map nos. G17, G18 and G26; Table 1). The Basalt of Sentinel Gap is subdivided in the Athena 7.5′ quadrangle into the following units:

Twfsl **Basalt of Sentinel Gap, low-phosphorous lava flows (middle or lower Miocene)** — Flow-on-flow sequence of high-titanium and lower-phosphorus basalt lava flows (SiO_2 = 51.28 to 53.22 weight percent; TiO_2 = 3.02 to 3.33 weight percent; P_2O_5 = 0.58 to 0.64 weight percent; n = 22 analyses) mapped at the top of the Sentinel Gap section in the Athena 7.5′ quadrangle (Plate 1; Figures 3a and 5; Tables 1 and 2). Thickness of unit **Twfsl** ranges between 50 and 74 m in the Athena 7.5′ quadrangle; the unit is ~74 m thick in water well UMAT 57710 at Athena (Plate 1, cross section A-A′).

Twfsh **Basalt of Sentinel Gap, high-phosphorous lava flows (middle or lower Miocene)** — Flow-on-flow sequence of high-titanium and higher-phosphorus basalt lava flows (SiO_2 = 51.56 to 52.83 weight percent; TiO_2 = 2.9 to 3.21 weight percent; P_2O_5 = 0.64 to 0.72 weight percent; n = 12 analyses) mapped beneath the low-phosphorus Sentinel Gap unit (**Twfsl**) in the Athena 7.5′ quadrangle (Plate 1; Figures 3a and 5; Tables 1 and 2). Thickness of unit **Twfsh** ranges between 30 and 60 m in the Athena 7.5′ quadrangle; the unit is ~48 m thick in water well UMAT 57710 at Athena (Plate 1, cross section A-A′).

Twfh **Basalt of Sand Hollow (middle or lower Miocene)** — Flow-on-flow sequence of high-titanium basalt lava flows (SiO_2 = 51.48 to 52.49 weight percent; TiO_2 = 2.84 to 3.1 weight percent; P_2O_5 = 0.55 to 0.61 weight percent; n = 10 analyses) mapped in the highlands east of the Thorn Hollow fault in the eastern part of the Athena 7.5′ quadrangle (Plate 1; Figures 3a and 5; Tables 1 and 2). West of the Thorn Hollow fault, the Basalt of Sand Hollow (**Twfh**) is only exposed beneath the Basalt of Sentinel Gap (**Twfsh**) along Wildhorse and Eagle creeks (Plate 1). The Basalt of Sand Hollow (**Twfh**) is distinguished from the underlying Basalt of Ginkgo (**Twfg**) and overlying basalt of Sentinel Gap (**Twfsl**, **Twfsh**) by higher amounts of chromium (avg. Cr = 36 ppm), lower titanium (avg TiO_2 = 2.95 weight percent) and phosphorus (avg. P_2O_5 = 0.57 weight percent), and higher magnesium (avg. MgO = 4.33 weight percent)(Figures 2 and 5; Tables 1 and 2). Thickness of unit **Twfh** is as much as 55 m on Reed and Hawley Mountain in the southeast part of the Athena 7.5′ quadrangle, ~79 m thick in water well UMAT 57710 at Athena (Plate 1, cross section A-A′), and as thick as 75 m at the confluence of Pine Creek and Dry Hollow in the Milton Freewater 7.5′ quadrangle (Figure 3a; Madin and others, 2023). Typical hand samples are pale blue (5B 6/2) to medium dark gray (N4) and aphyric to very sparsely porphyritic with 1 to 5 percent (vol.) yellow brown (5YR 5/6) to very pale orange (10YR 8/2) plagioclase phenocrysts and glomerophenocrysts up to 3 cm and ≤1 percent clinopyroxene microphenocrysts ≤1 mm, enclosed within a fine-grained equigranular, hypocrystalline groundmass of plagioclase, intergranular clinopyroxene, minor iron-titanium oxides, and intersertal to hyalophitic glass. Swanson and others (1981) mapped N25°W-striking dikes along Little Dry Creek that we correlate with the Basalt of Sand Hollow (**Twfh**) on the basis of texture and geochemistry (SiO_2 = 52.01 weight percent; TiO_2 = 2.86 weight percent; Cr = 36 ppm; n = 1 analysis; Plate 1, map no. G50; Table 1). The Basalt of Sand Hollow (**Twfh**) has normal magnetic polarity and an early to middle Miocene age between 16.1 and 15.9 Ma (Figure 2).

Twfg **Basalt of Ginkgo (middle or lower Miocene)** —High-titanium basalt lava flows (SiO_2 = 51.31 weight percent; TiO_2 = 3.08 weight percent; P_2O_5 = 0.7 weight percent; n = 1 analysis) mapped below the Basalt of Sand Hollow (**Twfh**) and above the basalt of Museum (**Tgsmu**) along Dry Creek in the northwest corner of the Athena 7.5′ quadrangle (Plate 1; Figures 3a and 5; Table 1). The Basalt of Ginkgo (**Twfg**) thins and does not crop out west of the northwest-striking Little Dry Creek fault; it has not been recognized in cuttings recovered and geochemically fingerprinted from water well UMAT 57710 in the city of Athena (Plate 1). It is distinguished from the overlying Basalt of Sand Hollow (**Twfh**) by lesser amounts of chromium (Cr = 10 ppm), higher titanium (TiO_2 = 3.08 weight percent) and phosphorus (P_2O_5 = 0.7 weight percent), and less magnesium (MgO = 4.24 percent)(Figures 2 and 5; Table 1). Unit **Twfg** is chemically similar to the overlying Basalt of Sentinel Gap (**Twfsl**, **Twfsh**), having comparable contents of titanium, phosphorus, and chromium; it is differentiated by stratigraphic position and a greater abundance of plagioclase phenocrysts (Figures 2 and 5; Table 1). Thickness of the Basalt of Ginkgo (**Twfg**) is about 15 m along Dry Creek (Plate 1). Typical **Twfg** hand samples are medium dark gray (N4) to dark gray (N2) and abundantly porphyritic and microporphyritic, containing ~3 to 5 percent (vol.) yellow brown (5YR 5/6) to very pale orange (10YR 8/2) plagioclase microphenocrysts, phenocrysts, and glomerocrysts ≤3 cm, distributed within an inequigranular holocrystalline groundmass of plagioclase, intergranular clinopyroxene, and minor iron-titanium oxides.The Basalt of Ginkgo (**Twfg**) has normal magnetic polarity and an early to middle Miocene age between 16.1 and 15.9 Ma (Figure 2). Baksi (2022) reported an ^{40}Ar/^{39}Ar plateau age of 16.12 ± 0.05 Ma for the Basalt of Ginkgo (**Twfg**).

Disconformity

Grande Ronde Basalt

The Grande Ronde Basalt is the thickest, most voluminous formation of the CRBG (Reidel and Tolan, 2013) and is the stratigraphically lowest exposed geologic unit in the Athena 7.5′ quadrangle (Plate 1, cross section A-A′). The formation spans at least four paleomagnetic zones and has been stratigraphically subdivided into four normal and reversed polarity magnetostratigraphic units (R1, N1, R2, N2) by Swanson and others (1979)(Figure 2). In the map area, the Sentinel Bluffs (**Tgsmu**, **Tgsmc**), Winter Water (**Tgww**), Indian Ridge (**Tgir**), and Ortley (**Tgo**) members crop out at the surface, east of the Thorn Hollow fault (Plate 1; Figure 2). The Buttermilk Canyon member (**Tgbc**) is recognized to be present near the base of the N2 magnetostratigraphic unit in water well UMAT 57710 at Athena (Plate 1; cross section A-A′; Figure 2). An undifferentiated succession of lava flows of the R2 and N1 magnetostratigraphic unit (**Tgu**), mapped to the south and east of the map area (Kuehn, 1995; Ferns, 2006a, b), underly the N2 magnetostratigraphic unit in the Athena 7.5′ quadrangle (Plate 1, cross section A-A′; Figure 2). Grande Ronde lava flows are generally monotonously fine-grained, aphyric, and texturally non-distinctive tholeiitic basalts and basaltic andesites, with relatively homogeneous chemical compositions (Table 1 and 2). The Grande Ronde Basalt is distinguished from the overlying Wanapum Basalt by the local presence of the intervening Vantage Member of the Ellensburg Formation, the conspicuous absence of large plagioclase phenocrysts and glomerocrysts, and significantly lesser titanium contents (Figure 5; Tables 1 and 2; Swanson and others, 1979; Hooper, 2000; Tolan and others, 2009).

Normal-polarity (N2) magnetostratigraphic unit

The N2 magnetostratigraphic unit is the youngest Grande Ronde Basalt magnetostratigraphic unit covering ~114,500 km², with an estimated volume of 24,600 cubic kilometers (km³)(Figure 2; Reidel and Tolan, 2013). Ages of N2 Grande Ronde units are bracketed by U-Pb dates of 16.066 ± 0.040Ma for ash from the overlying Vantage Horizon and 16.254 ± 0.034 Ma for ash between the Wapshilla Ridge and Meyers Ridge Members of the underlying R2 magnetostratigraphic unit (Figure 2; Kasbohm and Schoene, 2018). Subdivided in the Athena 7.5′ quadrangle into the following subunits:

Sentinel Bluffs Member

Sentinel Bluffs Member (lower Miocene) — Flow-on-flow sequence of high-magnesium basaltic andesite lava flows (SiO_2 = 53.29 to 55.67 weight percent; TiO_2 =1.72 to 2.14 weight percent; MgO = 4.19 to 5.2 weight percent; n = 19 analyses) mapped beneath the Frenchman Springs Member (**Twfsl**, **Twfsh**, **Twfh**, **Twfg**) and above the Winter Water Member (**Tgww**) in the Athena 7.5′ quadrangle (Plate 1; Figures 3a and 5; Tables 1 and 2). The Sentinel Bluffs Member (**Tgsmu**, **Tgsmc**) is distinguished from other members of the Grande Ronde Basalt in the map area on the basis of texture and lesser amounts of silica (avg. SiO_2 = 54.58 weight percent) and higher contents of magnesium (avg. MgO = 4.73 weight percent)(Figure 5; Tables 1 and 2). Thickness of the compound Sentinel Bluffs Member (**Tgsmu**, **Tgsmc**) in the map area is as much as 137 m beneath the city of Athena (water well UMAT 57710) and at Reed and Hawley Mountain (Plate 1, cross section A-A′). The compound unit (**Tgsmu**, **Tgsmc**) is ≤80 m thick along Dry Creek (Plate 1). Typical hand samples are medium light gray (N6) to medium gray (N5) and aphyric to very sparsely microporphyritic, containing ≤2 percent (vol.) clear plagioclase microphenocrysts ≤1 mm distributed within an equigranular, fine-grained diktytaxitic hypocrystalline groundmass of plagioclase, intergranular clinopyroxene, minor iron-titanium oxides, and intersertal glass. Olivine microphenocrysts are also present in some lava flows. The Sentinel Bluffs Member (**Tgsmu**, **Tgsmc**) has normal magnetic polarity and an early Miocene age of ~16.1 Ma (Figure 2). It is subdivided in the map area into the following units:

Tgsmu **Basalt of Museum (lower Miocene)** —Basaltic andesite lava flows (SiO_2 = 54.37 to 55.67 weight percent; TiO_2 =1.72 to 1.83 weight percent; MgO = 4.66 to 4.89 weight percent; n = 10 analyses) mapped at the top of the Sentinel Bluffs Member (**Tgsmu**, **Tgsmc**) in the Athena 7.5′ quadrangle (Plate 1; Figure 5; Tables 1 and 2). Distinguished from the underlying Basalt of McCoy Canyon (**Tgsmc**) on the basis of lesser contents of titanium (avg. TiO_2 = 1.76 weight percent)(Figures 2 and 5; Tables 1 and 2). Thickness of unit **Tgsmu** is as much as 45 m on Reed and Hawley Mountain in the southeast part of the Athena 7.5′ quadrangle; the unit is ~63 m thick in water well UMAT 57710 at Athena (Plate 1; cross section A-A′). Baksi (2022) reported an ^{40}Ar/^{39}Ar plateau age of 16.15 ± 0.07 Ma for the Basalt of Museum (**Tgsmu**).

Tgsmc **Basalt of McCoy Canyon (lower Miocene)** — Basaltic andesite lava flows (SiO_2 = 53.29 to 55.53 weight percent; TiO_2 =1.86 to 2.14 weight percent; MgO = 4.19 to 5.22 weight percent; n = 8 analyses) mapped below the Basalt of Museum (**Tgsmu**) in the Athena 7.5′ quadrangle (Figures 2, 3a, and 5; Tables 1 and 2). Distinguished from the overlying Basalt of Museum (**Tgsmu**) on the basis of higher contents of titanium (avg. TiO_2 = 1.93 weight percent)(Figures 2 and 5; Tables 1 and 2). Thickness of unit **Tgsmc** is as much as 85 m on Reed and Hawley Mountain in the southeast part of the Athena 7.5′ quadrangle; the unit is ~41 m thick in water well UMAT 57710 at Athena (Plate 1; cross section A-A′; Figure 3a).

Winter Water Member

Tgww **Winter Water Member (lower Miocene)** — Basaltic andesite lava flows (SiO_2 = 54.69 to 56.4 weight percent; TiO_2 = 2.1 to 2.38 weight percent; MgO = 3.23 to 3.48 weight percent; n = 9 analyses) cropping out below the Sentinel Bluffs Member (**Tgsb**) and above the Indian Ridge Member (**Tgir**) east of the Thorn Hollow fault in the Athena 7.5′ quadrangle (Plate 1; Figures 2, 3a, and 5; Tables 1 and 2). Unit **Tgww** is distinguished from the overlying Sentinel Bluffs Member (**Tgsb**) by lesser amounts of magnesium (avg. MgO = 3.36 weight percent) and from the underlying Indian Ridge Member (**Tgo**) by higher amounts of titanium (avg. TiO_2 = 2.22 weight percent)(Figures 2 and 5; Tables 1 and 2). Thickness of the Winter Water Member (**Tgww**) is as much as 52 m along Dry Creek in the northeast part of the Athena 7.5′ quadrangle; the unit has a similar thickness of 55 m in water well UMAT 57710 at Athena (Plate 1, cross section A-A′; Figure 3a). Typical hand samples of the Winter Water Member (**Tgww**) are medium dark gray (N4) to dark gray (N2), aphyric to very sparsely microporphyritic and glomeroporphyritic, containing 1 to 2 percent (vol.) clear, euhedral, prismatic plagioclase microphenocrysts and v-shaped or radial, spoked glomerocrysts <2 mm across, contained within an inequigranular hypocrystalline groundmass of plagioclase, intergranular clinopyroxene, intersertal glass, and minor iron-titanium oxides. The Winter Water Member (**Tgww**) has normal magnetic polarity and an early Miocene age of ~16.1 Ma (Figure 2).

Indian Ridge Member

Tgir **Indian Ridge Member (lower Miocene)** — Basaltic andesite lava flow (SiO_2 = 53.1 to 53.46 weight percent; TiO_2 = 1.69 to 1.98 weight percent; MgO = 4.67 to 5.42 weight percent; n = 7 analyses outside map area) cropping out below the Winter Water Member (**Tgww**) east of the Saddle Hollow fault along Pine Creek (Plate 1) and along Dry Creek, 0.8 km east of the Athena 7.5′ quadrangle (Figures 2, 3a, and 5; Table 1). Unit **Tgir** is distinguished from the overlying Winter Water Member (**Tgww**) and underlying Ortley member (**Tgo**) by less amounts of silica (avg. SiO_2 = 53.23 weight percent) and higher amounts of magnesium (avg. MgO = 4.91 weight percent)(Figures 2 and 5; Table 1). The Indian Ridge Member (**Tgir**) also contains notably less amounts of titanium (avg TiO_2 = 1.92 weight percent) than the Winter Water Member (**Tgww**). Thickness of the Indian Ridge Member (**Tgir**) is as much as 38 m at Blalock Mountain in the Bowlus Hill 7.5′ quadrangle (Figure 3a; Madin and others, 2023). Typical hand samples of the Indian Ridge Member (**Tgir**) are medium dark gray (N4) to dark gray (N2), aphyric to very sparsely microporphyritic, containing 1 to 2 percent (vol.) clear, euhedral, prismatic plagioclase microphenocrysts <2 mm across, contained within an inequigranular hypocrystalline groundmass of plagioclase, intergranular clinopyroxene, intersertal glass, and minor iron-titanium oxides. The Indian Ridge Member (**Tgir**) has normal magnetic polarity and an early Miocene age of ~16.1 Ma (Figure 2).

Ortley member

Tgo **Ortley member (lower Miocene)** — Basaltic andesite lava flow (SiO_2 = 56.23 to 57.41 weight percent; TiO_2 =1.74 to 1.94 weight percent; MgO = 3.49 to 4.32 weight percent; n = 6 analyses outside map area) mapped below the Indian Ridge Member (**Tgir**), east of the Saddle Hollow fault along Pine Creek (Figure 2; Plate 1). Unit **Tgo** is distinguished from the overlying Winter Water Member (**Tgww**) and from the underlying Buttermilk Canyon member (**Tgbc**) by higher amounts of silica (avg SiO_2 = 56.89 weight percent) and less amounts of titanium (avg. TiO_2 = 1.86 weight percent)(Figures 2 and 5; Table 1). Thickness of the Ortley member is as much as 45 m. Typical hand samples are medium dark gray (N4) to medium bluish gray (5B 5/1), aphyric to very sparsely microporphyritic, containing 1 to 2 percent (vol.) euhedral, prismatic, clear plagioclase micophenocrysts <1 mm across contained within a locally diktytaxitic, equigranular very fine-grained hypocrystalline groundmass of plagioclase, intergranular clinopyroxene, intersertal glass, and minor iron-titanium oxides. The Ortley member (**Tgo**) has normal magnetic polarity and an early Miocene age of ~16.1 Ma (Figure 2).

Buttermilk Canyon member

Tgbc **Buttermilk Canyon member (lower Miocene)(cross-section only)** — Basaltic andesite lava flow (SiO_2 = 52.57 to 55.79 weight percent; TiO_2 = 2.08 to 2.68 weight percent; MgO = 3.37 to 3.71 weight percent; n = 7 analyses [5 outside map area])(Figures 2 and 5; Table 2). The Buttermilk Canyon member (**Tgbc**) does not crop out at the surface in the Athena 7.5′ quadrangle but is recognized to be present in a faulted stratigraphic sequence below the Winter Water Member (**Tgww**) at Athena based on geochemical correlation with samples UMAT 57710-1420 and UMAT 57710-1520 collected from water well UMAT 57710 (Plate 1, cross section A-A′; Figure 3a). In the greater Athena area, the Buttermilk Canyon member (**Tgbc**) has been mapped beneath the Ortley member (**Tgo**) at Blalock Mountain in the southeast part of the Bowlus Hill 7.5′ quadrangle and geochemically identified in the lower part of the N2 magnetostratigraphic unit in the Thorn Hollow 7.5′ quadrangle (Figure 3a; Ferns, 2006b; Madin and others, 2023). Unit **Tgbc** is distinguished from the overlying Ortley member (**Tgo**) by less amounts of silica (avg. SiO_2 = 54.30 weight percent) and higher amounts of titanium (avg. TiO_2 = 2.17 weight percent). Thickness of the Buttermilk Canyon member (**Tgbc**) is as much as 23 m at Blalock Mountain (Madin and others, 2023); the unit is ~41 m thick in water well UMAT 57710 at Athena (Plate 1; cross section A-A′; Figure 3a). Typical hand samples are medium dark gray (N4) and aphyric to very sparsely microporphyritic, containing <1 percent (vol.) euhedral, prismatic, clear plagioclase micophenocrysts ≤2 mm (0.1 in) across contained within a locally diktytaxitic, equigranular, very fine-grained hypocrystalline groundmass of plagioclase, intergranular clinopyroxene, intersertal glass, and minor iron-titanium oxides. TThe Buttermilk Canyon member (**Tgbc**) has normal magnetic polarity and an early Miocene age of ~16.1 Ma (Figure 2).

Reversed-polarity (R2) magnetostratigraphic unit/Normal-polarity (N1) magnetostratigraphic unit

The R2 magnetostratigraphic unit is the most aerially extensive and most voluminous of the four Grande Ronde Basalt magnetostratigraphic units covering ~117,730 km², with an estimated volume of 56,000 km³ (Figure 2; Reidel and Tolan, 2013). The older N1 magnetostratigraphic unit covers ~102,400 km² and has an estimated volume of 24,600 km³, the smallest volume of the four Grande Ronde Basalt magnetostratigraphic units (Reidel and Tolan, 2013). Kasbohm and Schoene (2018) reported ages for the R2 magnetostratigraphic unit of 16.288 ± 0.046 Ma and 16.210 ± 0.047 Ma and early Miocene ages between ~16.572 and 16.288 Ma for the N1 magnetostratigraphic unit (Figure 2). Baksi (2022) stated ^{40}Ar/^{39}Ar plateau ages of 16.43 ± 0.04 Ma and 16.44 ± 0.06 Ma for the middle and lower parts of the R2 unit magnetostratigraphic unit, and an ^{40}Ar/^{39}Ar plateau age of 16.43 ± 0.09 Ma for the uppermost part of the N1 magnetostratigraphic unit, placing the R2-N1 boundary in the Grande Ronde Basalt at ~16.45 Ma.

Tgu **Grande Ronde Basalt, undivided (lower Miocene) (*cross section only)*** — Older Grande Ronde Basalt lava flows (**Tgu**) lying stratigraphically below the N2 magnetostratigraphic unit but not exposed in the Athena 7.5′ quadrangle (Plate 1, cross section A-A′; Figure 3a). Geologic mapping east and south of Athena shows unit **Tgu** is likely to include both lava flows of the R2 magnetostratigraphic unit (e.g., Grouse Creek and Wapshilla Ridge members) and older lava flows of the N1 magnetostratigraphic unit (Figure 3a; Kuehn, 1995; Ferns, 2006a,b; Ferns and McConnell, 2006; Madin and others, 2023). The R2 magnetostratigraphic unit is 150 to 200 m thick south and east of the Athena area (Ferns, 2006a), thickening northward to at least 530 m north and east of Athena (Kuehn, 1995).

OTHER ROCKS

Tfb **fault breccia (upper to middle Miocene [?])** — Brecciated rock crosscutting CRBG lava flows between strands of the Saddle Hollow fault, north of Wildhorse Creek in the southeast corner of the Athena 7.5′ quadrangle (Plate 1; Figure 3a). The main zone of breccia is as wide as 90 m and chiefly composed of intensely damaged, poorly sorted, clast-supported, angular basalt fragments ranging from < 1 cm to > 10 cm across (Plate 1). Fault breccia (**Tfb**) is assigned a middle(?) to late Miocene age based on major fault movement postdating the 15.9 to 16.1 Ma Basalt of Sentinel Gap (**Twfsl**)(Plate 1, cross section A-A′).

Table 1. Select geochemical analyses for Columbia River Basalt Group lava flows and dikes in the Athena 7.5′ quadrangle.

Table 2. Geochemical analyses for Columbia River Basalt Group lava flows in water well UMAT 57710 in the Athena 7.5′ quadrangle.

Sample	UMAT 57710-0080	UMAT 57710-0270	UMAT 57710-0380	UMAT 57710-0480	UMAT 57710-0580	UMAT 57710-0650	UMAT 57710-0760	UMAT 57710-0860	UMAT 57710-1110	UMAT 57710-1180	UMAT 57710-1281	UMAT 57710-1420	UMAT 57710-1520	UMAT 57710-1560
Geographic Area	City of Athena	City of Athena	City of Athena	City of Athena	City of Athena	City of Athena	City of Athena	City of Athena	City of Athena	City of Athena	City of Athena	City of Athena	City of Athena	City of Athena

Metric to Common English Conversion

Multiply	By	To obtain
millimeter (mm)	0.039	inch
centimeter (cm)	0.394	inch
meter (m)	3.281	feet
meter (m)	1.094	yard
kilometer (km)	0.621	mile
square kilometer (km²)	0.386	square mile
cubic kilometer (km³)	0.240	cubic mile

Expires: 12/1/2023

Figure 5. Weight percent phosphorus (P_2O_5) versus titanium (TiO_2) variation diagram for the CRBG . The "titanium gap" is after Seims and others (1974). Data shown includes 367 CRBG analyses from the Athena, Adams, Milton Freewater, and Bowlus Hill 7.5′ quadrangles reported in this publication, Bush and others (1973), Kuehn (1995), Hutter (1997), Madin and others (2023), and McClaughry (2021, unpublished data). Symbol colors are keyed to colors used for the geologic map units on Plate 1. Additional units shown in legend are from Madin and others (2023): **Twlg** – Lookingglass Member; **Tggc** – Grouse Creek Member.